the precise molecular mechanisms underlying TCDD toxicity remain to be established (11–15).

Although several previous studies analyzed the gene expression profiles of hepatocyte cell line cells treated with TCDD using cDNA array (16, 17), no studies so far used an unbiased comprehensive gene expression profiling approach to *in vivo* materials. Serial analysis of gene expression (SAGE), first described by Velculescu *et al.* (18), has the potential to detect all genes expressed in a given material with quantitative information by generating a transcript profile relying on 14 bps cDNA sequence (SAGE tag) for gene identification. To identify the genes that are regulated by TCDD and possibly involved in hepato-toxicity or hepatochemocarcinogenesis, we have applied SAGE technique to take advantage of a normalization step and identification of novel genes, and the mouse model treated by oral TCDD administration to reflect *in vivo* delicate response to TCDD.

## MATERIALS AND METHODS

*Tissue collection.* C57BL/6 female mice were purchased from SLC (Shizuoka, Japan) at 5-week-old and were allowed 1 week for acclimatization. At six weeks of age, a single oral dose of 20 $\mu$g TCDD/kg body weight dissolved in DMSO was administered. The control group received the vehicle only. Seven days after TCDD administration, whole livers from four control female and three TCDD-treated female mice were collected and stored in liquid nitrogen until use. This study was conducted according to the guidelines of the National Institute for Environmental Studies.

*SAGE.* Total RNA was isolated from each homogenized sample separately using RNA ZolB (TEL-Test, Inc., Friendswood, TX) following manufacturer's instruction. Polyadenylated mRNA was isolated by $\mu$MACS mRNA Isolation Kit (Miltenyi Biotech., GmbH Bergisch Gladbach, Germany) and quantified by spectrophotometry, and then equal amounts of mRNA from each liver were used to make two pools (vehicle-treated group and TCDD-treated group). Four micrograms of mRNA was used to construct each SAGE library according to SAGE protocol version 1.0e (http://www.sagenet.org/sage_protocol.htm).

Briefly, polyadenylated RNA was converted to double-strand complementary DNA (cDNA) by the SuperScript Choice System (Gibco BRL, Grand Island, NY) with a 5'-biotinylated oligo $dT_{18}$ primer. Double stranded cDNA was cleaved with *Nla* III and the 3'-terminal cDNA fragments were trapped to Dynabeads M-280-streptavidin (Dynal, Oslo, Norway). After ligation of the oligonucleotides containing recognition sites for *Bsm*F I, the bound cDNA was released from the beads by digestion with *Bsm*F I. SAGE tag overhangs were filled with Klenow enzyme, and the tags from the two pools were combined and ligated to each other. The ligation product was amplified with PCR, concatemerized and cloned into the *Sph* I site of pZero-1 (Invitrogen, Carlsbad, CA). Samples were sequenced with BigDye terminator kit version 2 and analyzed by 96 lane ABI 377 automated sequencer (Perkin-Elmer, Branchberg, NJ). Sequence files were analyzed by means of the SAGE program group and DNAsis software (Takara, Osaka, Japan). After correcting sequencing mistakes, a total of tags representing 56,420 and 56,647 tags from control and TCDD treated mouse livers were analyzed. Tag sequence was examined by use of the BLAST at NCBI (http://www.ncbi.nlm.nih.gov/blast/). Statistical significance was calculated by critical ratio.

*RT-PCR.* Total RNA was extracted using RNAzolB (TEL-Test, Inc.). Three micrograms of total RNA was reverse transcribed in a total of 100 $\mu$L of reaction solution including 240 units of Moloney murine leukemia virus reverse transcriptase (Sawady Technology Co., Tokyo, Japan), 80 units of RNase inhibitor (Sawady Technology Co.), 50 mmol/L Tris-HCl, 125 mmol/L KCl, 8 mmol/L $MgCl_2$, 10 mmol/L dithiothreitol (Gibco BRL), 1 mmol/L deoxyribonucleotide triphosphates, and 2 mmol/L random hexamer (Promega Co., Madison, WI) for 1 h at 42°C. PCR was performed in 20 $\mu$L of mixture containing 0.5 units of AmpliTaq DNA polymerase (PE Biosystems), 10 mmol/L Tris-HCl, 6.5 mmol/L $MgCl_2$, 1 mmol/L deoxyribonucleotide triphosphates, and 0.5 $\mu$mol/L sense and antisense primers by use of a Perkin-Elmer DNA thermal cycler. Primer sequences were as follows. GAPDH: sense 5'-CCTTCATTGACCTCAACTAC-3', antisense 5'-TCACTACCGTACCTGACACCA-3'; CTP 1al: sense 5'-GCCTCATTGAGCATTGTCAGG-3', antisense 5'-TGCCCAAACCAAAGAGAGTGA-3'; histidine ammonia lyase: sense 5'-CACAGGTTCTGCGATCGTGTT-3', antisense 5'-CACAGATGAAGGGTGGCACAG-3'; interferon-inducible GTPase: sense 5'-CTCTGTGGGTGGCACCATTC-3', antisense 5'-ATGTGGCAGGATAGCTGGCC-3'; EST, RIKEN cDNA 0610011L04 gene: sense 5'-AGAAGCTCCCGTCCGTGTTC-3', antisense 5'-CCATTTCTTTTAAGGCCTCCG-3'; EST, similar to DKFZp564p1263.1: 5'-GCTTTCCTCTCCTGTGGTGGA-3', 5'-GCCTGAGACCCTTTTCCTTGG-3'. The cycle profile of PCR was as follows: denature at 94°C for 45 s, annealing at 57°C for 45 s, and extension at 72°C for 1 min. Twenty-eight cycles of PCR amplification were performed to compare the gene expression levels of each sample.

## RESULTS

### *SAGE Profiles*

Total of 56,420 tags from normal mouse liver and 56,647 tags from TCDD-treated liver library were sequenced and analyzed. These tags corresponded to 14,117 and 15,696 unique transcripts, respectively. Of the 24,058 different transcripts in total observed in these libraries, 14,555 tags (60.5%) matched to existing known expressed sequences [Table 1]. Of total matched tags, 3,086 tags (21.2%) matched more than one sequences located in different Unigene clusters. Only 109 tags (0.5%) were expressed in more than 100 counts; 6,596 tags (27.4%) between 9 to 2 counts, whereas 16,093 tags (66.9%) as a single count. This demonstrates that most of the genes identified in each library were expressed at low levels. The outline of tag distribution in normal liver was similar to that in human liver (19).

### *Abundant Transcripts*

Table 2 shows the 50 most expressed tags in the normal mouse liver, in comparison with these in the normal human liver (19). The genes encoding plasma proteins such as albumin, transthyretin, apolipoproteins and coagulation factor were highly expressed in the normal mouse liver as in the human liver. This indicates that mouse liver also constantly synthesizes these plasma proteins and their composition is quite similar except for several mouse-specific genes such as major urinary proteins (MUPs) and hepcidin.

TABLE 1

Distribution of 24,058 Unique SAGE Tags in the Mouse Liver Libraries

| | SAGE tag frequencies | | | | | |
|---|---|---|---|---|---|---|
| | 100> | 99 to 10 | 9 to 5 | 4 to 2 | 1 | Total |
| Total unique tags* | 109 (0.5) | 1260 (5.2) | 1443 (6.0) | 5153 (21.4) | 16093 (66.9) | 24058 (100) |
| Total matched tags† | 107 (98.2) | 1147 (91.0) | 1250 (86.6) | 3887 (75.4) | 8164 (49.3) | 14555 (60.5) |
| Single matched tags§ | 90 (84.1) | 938 (81.8) | 999 (79.9) | 3049 (78.4) | 6393 (78.3) | 11469 (78.8) |
| Multiple matched tags§ | 17 (15.9) | 209 (18.2) | 251 (20.1) | 838 (21.6) | 1771 (21.7) | 3086 (21.2) |

* The number in parentheses is the percentage of tags in the total unique tag set.
† The number in parentheses is the percentage of the tags in the total tags of each subgroup.
§ The number in parentheses is the percentage of tags within the total matched tags.

*Identification of TCDD Responsive Genes*

Treatment of mice with TCDD resulted in the change of the expression of 346 unique transcripts including 94 ESTs ($p < 0.05$) [Fig. 1]. SAGE data are available at our homepage (http://www.prevent.m.u-tokyo.ac.jp). Table 3 shows the 56 unique transcripts significantly affected by TCDD treatment ($p < 0.01$). Of these, 25 transcripts were up-regulated and 31 transcripts were down-regulated. The genes intensively up-regulated include metallothioneins (MTs), albumin, heat shock protein 70, *CYP1a2,* and the genes down-regulated include apolipoproteins, complements and enzymes related to cellular metabolism. Of 346 transcripts affected by TCDD treatment ($p < 0.05$), approximately 150 tags were single-matched to named transcripts. Table 4 shows classified transcripts responsive to TCDD treatment ($p < 0.05$). Not only gene expression of enzymes related to xenobiotics metabolism or stress, but also the expression of wide-range of the genes encoding plasma proteins, transcription factors and signal transduction molecules was affected by TCDD treatment.

*Validation of SAGE Tag Representation*

To verify that the SAGE data strictly reflected the changes in gene expression, RT-PCRs were performed on the identical samples from normal mouse liver and TCDD-treated liver [Fig. 2]. The six representative genes (ESTs, histidine ammonia lyase, interferon-inducible GTPase, *CYP 1a1* and GAPDH) were evaluated. The expression levels of each gene were well correlated to the corresponding SAGE tag abundance, demonstrating that our SAGE analysis accurately reflected the transciprome of normal and TCDD-treated mouse liver.

## DISCUSSION

*Comparison between Mouse and Human Liver Transcriptome*

In this study, we have sequenced total of 113,067 tags, including 56,420 tags and 56,647 tags from normal mouse liver and TCDD-treated liver library, respectively. This enabled us to perform direct comparison between normal mouse and normal human liver SAGE (19). The overall gene expression profiles between normal mouse and human liver were quite similar, indicating that mouse liver resembles to human liver in functional aspects, and therefore mouse liver could serve as a substitute for human liver in toxicological study. Strong similarity of the results between mouse and human liver transcriptomes may also suggest high stability and reproducibility of our SAGE analysis and usefulness of SAGE method to compare the gene expression profiles of the same organ in different species.

However, there were some differences in gene expression profiles between mouse and human liver. Several serum proteins such as major urinary proteins (MUPs) and hepcidins were specifically and highly expressed in the mouse liver. MUPs are reported to be synthesized in the liver, bind volatile signaling pheromones and be secreted into urine (20, 21). The overall abundance of MUPs family in the liver transcriptome was 2.399% in this study. This finding supports that MUPs play an important role in the individual recognition that is particularly essential to rodents. In addition, the fact that the expression of MUPs was up-regulated by TCDD treatment indicates that MUPs might be generally induced by stress to lead to the actions for species conservation.

Hepcidins, cystein-rich antimicrobial peptides, are synthesized in the liver and thought to participate in innate immunity. Previous study reported that hepcidins mRNA expression was enhanced in mouse hepatocytes in response to LPS and exhibited antifungal and antimicrobial activity (22). There are similar antimicrovial peptides including alpha- and beta-defensins and protegrins in mammals, but high basal level of hepcidins mRNA expression, which accounts for 0.3775% abundance of total liver transcripts in our study, suggests that hepcidins may also play an important role in innate immunity in mice. Interestingly, gene expression of hepcidins was down-regulated by

TABLE 2

The 50 Most Expressed Tags in the Normal Mouse Liver, in Comparison with the Normal Human Liver

| Mouse liver | | | | | Human liver | | | | |
|---|---|---|---|---|---|---|---|---|---|
| Count | Abundance | Tag sequence | Unigene | Description | Count | Abundance | Tag sequence | Unigene | Description |
| 2516 | 4.4594 | AAGACTCAGG | 16773 | Serum albumin variant | 1123 | 3.5772 | AGAATAAGAG | 184411 | Albumin |
| 1803 | 3.1956 | GCTGCCCTCC | 142188 | Delta-like homolog (Drosophila) | 904 | 2.8796 | TGGACGCGCT | 93194 | Apolipoprotein A-I |
| 925 | 1.6394 | CATCGCCAGT | 21417 | Apolipoprotein E | 797 | 2.5388 | TGGCCCCAGG | 268571 | Apolipoprotein C-I |
| 861 | 1.526 | AATTTCTTCC | 157893 | Major urinary protein 1/2 | 690 | 2.1979 | CTGGCCTCCC | 73849 | Apolipoprotein C-III |
| 679 | 1.2034 | GTGGCTCACA | | Multiple match | 483 | 1.5386 | CACCTAATTG | | ATPase 6/8 |
| 639 | 1.1325 | AGTCCACTGG | | Multiple match | 358 | 1.1404 | TGATTTCACT | | Cytochrome oxidase 3 |
| 620 | 1.0989 | TGCCCAGGGA | 7010 | Alpha-2-HS-glycoprotein | 357 | 1.1372 | CCCATCGTCC | | Cytochrome oxidase 2 |
| 566 | 1.0031 | ACTGATTATG | 43677 | Apolipoprotein A-II | 336 | 1.0703 | GGAAAAGTGG | 297681 | Proteinase inhibitor 1, AT1 |
| 504 | 0.8933 | CCCTGAGGGG | 37214 | Protein that interacts with C kinase 1 | 303 | 0.9652 | CGACCCCACG | 169401 | Apolipoprotein E |
| 473 | 0.8383 | ATACTGACAT | 142740 | Metallothionein 2 | 303 | 0.9652 | ACTTTTTCAA | | No reliable match |
| 408 | 0.7231 | CTGGAGACGC | 26743 | Apolipoprotein A-I | 301 | 0.9588 | TTCATACACC | | NADH dehydrogenase 4 |
| 356 | 0.6309 | ATGACTGATA | | No reliable match | 300 | 0.9556 | GCCGGGCCCT | 2257 | Vitronectin, somatomedin B, S-protein |
| 335 | 0.5937 | ACCTTGGAAG | 28897 | Apolipoprotein CI | 300 | 0.9556 | TGTACCTCAG | 572 | Orosomucoid 1 |
| 330 | 0.5848 | AATTCGCGGA | 2108 | Transthyretin | 283 | 0.9015 | GTGGGCACCT | 76461 | Retinol-binding protein 4, plasma |
| 321 | 0.5689 | ACATTGGGCG | 22126 | Fatty acid binding protein 1, liver | 277 | 0.8824 | TGTGGAGAGC | 237658 | Apolipoprotein A-II |
| 303 | 0.537 | AGGAGGACTT | | Multiple match | 248 | 0.79 | GGCAACGGTA | | Multiple match |
| 282 | 0.4998 | GATGAGACAG | 89363 | Serine protease inhibitor 1-3 | 242 | 0.7709 | CTAAGGTGGT | 1252 | Apolipoprotein H (beta-2-glycoprotein I) |
| 273 | 0.4838 | AGCAGTCCCC | 99535 | Mitochondrial DNA | 241 | 0.7677 | TCTAAGTACC | 75990 | Haptoglobin |
| 253 | 0.4484 | GAAATTCTCC | | Major urinary protein 1/3 | 234 | 0.7454 | CACTACTCAC | | Cytochrome b |
| 242 | 0.4289 | ATAATACATA | 142740 | Metallothionein 2 | 226 | 0.7199 | TAACCAAGAG | 194366 | Transthyretin |
| 240 | 0.4253 | GAGAGGCCCT | 89481 | Major urinary protein 1 | 218 | 0.6944 | CCCTGGGTTC | 111334 | Ferritin, light polypeptide |
| 233 | 0.4129 | CCCTGGGTTC | 7500 | Ferritin light chain 1 | 200 | 0.6371 | CTAAGACTTC | | 16S rRNA, mitochondrial |
| 219 | 0.3881 | AGGACAAATA | | Mitochondrial DNA | 195 | 0.6212 | AGCCCTACAA | | NADH dehydrogenase 3 |
| 213 | 0.3775 | ATGGCACTCA | 23995 | Hepcidin antimicrobial peptide | 168 | 0.5352 | ATTTGAGAAG | | Cytochrome oxidase 1 |
| 211 | 0.3739 | GGGAGAGTGG | 30025 | Antithrombin-III | 166 | 0.5288 | ACCCTTGGCC | | NADH dehydrogenase 1 |
| 207 | 0.3668 | GTGGAGAAAC | 4205 | Group specific component | 149 | 0.4746 | CTCCAGAATA | 234234 | Aldolase B, fructose-bisphosphate |
| 203 | 0.3598 | TGGGGCCTCT | 19131 | Complement component 3 | 149 | 0.4746 | TCGAAGCCCC | | No reliable match |
| 192 | 0.3403 | TATCTGTGCA | 22699 | Selenoprotein P, plasma, 1 | 145 | 0.4619 | TGTGCTGAAC | 284176 | Transferrin |
| 182 | 0.3225 | AGGCAGACAG | 16317 | Translation elongation factor 1 alpha 1 | 142 | 0.4523 | AAAACATTCT | | No reliable match |
| 173 | 0.3066 | TCCAAGCACG | 30063 | Ribonuclease, RNase A family 4 | 129 | 0.4109 | GTTGTCTTTG | 284394 | Complement component 3 |
| 173 | 0.3066 | CTGTCCCTAA | 2180 | Heat shock protein, 84 kDa 1 | 128 | 0.4077 | ACTAACACCC | | No reliable match |
| 169 | 0.2995 | TCACCCAATA | 87581 | Fibronectin 1 | 119 | 0.3791 | CATTTCAATA | 75431 | Fibrinogen, gamma polypeptide |
| 169 | 0.2995 | GTGCAAACTC | 16422 | ESTs, highly similar to fibrinogen gamma-a and | 119 | 0.3791 | GATCCCAACT | 118786 | Metallothionein 2A |
| 164 | 0.2906 | AACGTGCAGG | 3217 | Argininosuccinate synthetase 1 | 108 | 0.344 | CAAGCATCCC | | No reliable match |
| 164 | 0.2906 | GCCACGCCCC | 6584 | 4-Hydroxyphenylpyruvic acid dioxygenase | 106 | 0.3377 | TTGGTCCTCT | 324406 | Ribosomal protein L41 |
| 150 | 0.2658 | TCAGGCTGCC | 1776 | Ferritin heavy chain | 104 | 0.3313 | AGTCTGGCCT | 346935 | Hemopexin |
| 145 | 0.257 | AGCAATTCAA | 156913 | No reliable match | 103 | 0.3281 | CCTGTAATCC | | Multiple match |
| 144 | 0.2552 | GTGTGCCAGG | 3667 | Vitronectin | 98 | 0.3122 | GCAAGCCAAC | | No reliable match |
| 143 | 0.2534 | TGGGTTGTCT | 254 | Translationally regulated transcript (21 kDa) | 97 | 0.309 | GGCAGAGTAG | 75599 | Serine proteinase inhibitor, member 1 |
| 142 | 0.2516 | GCGATGAAAT | 88078 | Esterase 1 | 91 | 0.2899 | CAACTAATTC | 75106 | Clusterin |
| 141 | 0.2499 | AGAGTCACTG | 2605 | Retinol binding protein 4, plasma | 90 | 0.2867 | GTAGGCTGAG | 76730 | EST, KIAA0301 protein |
| 138 | 0.2445 | TGGATGCCTT | 2409 | Alcohol dehydrogenase 1, complex | 89 | 0.2835 | GTGAAACCCC | | Multiple match |
| 136 | 0.241 | CACATAAGAC | 10565 | Serine protease inhibitor 2 | 82 | 0.2612 | TGTGTTGAGA | 181165 | Eukaryotic translation elongation factor 1 |
| 127 | 0.225 | GAAGAGGGGG | 26730 | Haptoglobin | 81 | 0.258 | CCGTGCTCAT | 9857 | Carbonyl reductase |
| 126 | 0.2233 | TGTCTATTTC | 88793 | Fibrinogen, gamma polypeptide | 78 | 0.2485 | TTAAATGGAA | 90765 | Fibrinogen A |
| 118 | 0.2091 | TATTCTGCCC | 30061 | Alpha-2-glycoprotein 1, zinc | 76 | 0.2421 | TAAGCCCCGC | 2899 | 4-Hydroxyphenylpyruvate dioxygenase |
| 116 | 0.2056 | GGATCATCTC | 21193 | Cytochrome P450, steroid inducible 3a11 | 73 | 0.2325 | ACTTTCCAAA | | No reliable match |
| 112 | 0.1985 | CTCAGGCAAT | 29395 | Glycine N-methyltransferase | 72 | 0.2294 | GAGGCCAAGA | 89552 | Glutathione S-transferase A2 |
| 110 | 0.1949 | TCGGACCATA | 2197 | Alpha 1 microglobulin/bikunin | 71 | 0.2262 | AGCCTCCCGG | 144567 | Alanine-glyoxylate aminotransferase |
| 109 | 0.1931 | ATCACTTCCT | 14719 | Glutathione S-transferase, alpha 3 | 67 | 0.2134 | GTTGTGGTTA | 75415 | Beta-2-microglobulin |
| 56420 | | Total collected tags from normal mouse liver library | | | 31393 | | Total collected tags from normal human liver library | | |

*Note.* The numbers of detected tag copies from normal mouse liver SAGE library are shown in left column. The numbers of abundance are calculated as the numbers of tag copies divided by the numbers of total sequenced tags (56,420 tags). Normal human liver data are cited from our previous report (19). Further information on mouse liver SAGE library is available in our homepage, http://www.prevent.m.u-tokyo.ac.jp.

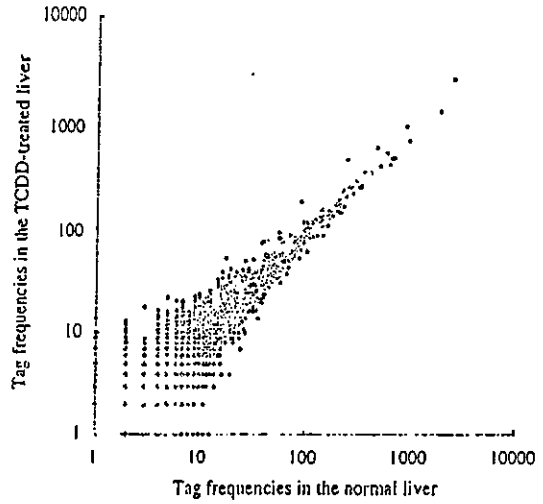


FIG. 1. Scatter plot analysis of the observed 27,726 different tags detected in total of 113,067 tags from the normal and TCDD-treated mouse liver SAGE library. The majority of the tags were expressed at similar level in the two samples (gray circle); however, there were 346 tags with statistically significant differences ($p < 0.05$) between normal and TCDD-treated mouse liver SAGE library (black circle).

TCDD treatment. Although previous studies indicated that immunotoxicity induced by TCDD is mainly caused by thymus atrophy and deterioration of T cell mediated immunity (23), our finding suggests that TCDD could also affect innate immunity by suppressing the gene expression of antimicrovial peptides.

*Genes Responsive to TCDD*

To facilitate evaluation of the gene expression changes by TCDD treatment from a biological perspective, the transcripts were also categorized by functional aspects. Although it is difficult to discuss each change in detail, several points can be made about how these data may suggest how TCDD-promoted transcriptional changes contribute to hepatic function.

*Signal transduction.* Rab proteins, members of the Ras superfamily of small GTPases, are key regulators of protein transport and seem to be involved in all aspects of vesicle trafficking (24, 25). Suppression of Rabs may influence an exocytosis of synthesized proteins and endocytosis of waste in the blood, that are the most fundamental functions of the liver, and lead to hepatocyte dysfunction.

Insulin-like growth factor binding proteins (IGFBPs), which are mainly synthesized in the liver, make complex with approximately 80–90% of circulating insulin-like growth factors (IGFs). Decrease in IGFBPs production results in an excess of bioactive IGFs and may potentiate the mitogenic effects of IGFs in hepatocarcinogenecity (26). Changes in the expression of these genes are likely to have major consequences in the regulation of cell growth and responses to external stimuli, and may contribute significantly to the carcinogenic potential of TCDD.

*Protein trafficking.* Changes of gene expression in this cluster may also contribute to functional deterioration of hepatocytes. Metaxin 2 is bound to the cytosolic face of the mitochondrial outer membrane with membrane bound metaxin 1 and thought to play a role in protein transport into mitochondria. Alteration of metaxin 2 gene expression may result in mitochondrial dysfunction.

*Transcription factors.* Activation and suppression of the expression of the genes encoding transcription factors are conspicuous characteristics of the TCDD action (27). TCDD altered the expression of at least 20 genes encoding transcription factors ($p < 0.05$). Although all of these changes may not be primary effects of TCDD, it is noteworthy that TCDD altered the expression of so many genes encoding transcription factors which might lead to extensive gene expression alterations in the downstream.

*Metabolic enzymes.* It was revealed that TCDD affected the expression of metabolic enzymes related to cellular energy, carbohydrates, lipids, and amino acid metabolisms as well as drug metabolizing enzymes. Prolonged alterations of these enzymes essential to liver function may lead to hepatic dysfunction and impairment of incomings and outgoings of energy metabolism and subsequent wasting syndrome. Besides *CYP 1A* and *1B* groups which are well-known TCDD-responsive genes, gene expression of *CYP 2d10* which is also known as testosterone 16 alpha hydroxylase was also found to be TCDD-responsive. In addition to testosterone, progesterone and estradiol are hydroxylated specifically at the 16 alpha position by *CYP 2d10* (28, 29). Thus the induction of this enzyme may cause changes of serum sex steroid hormone activity. So far estrogen-like effect on target tissues has been the central issue of TCDD toxicity (30), our result suggests that induction of CYP enzymes may indirectly disturb endocrine axis through deterioration of serum sex steroid hormone activity.

*Molecules related to cell damage, apoptosis and stress.* Cellular damage engages two fundamental cellular responses: apoptosis and the induction of heat shock proteins (Hsps) (31). The coordinated balance between these two opposing pathways governs the ultimate fate of the cell. The Hsps regulate the activity of multiple intracellular signaling intermediates, many of which are intimately involved in the execution of the apoptotic signaling pathways. In this study, Hsp70, one of the representative antiapoptotic Hsps, and Hsp10 were strongly induced, indicating that Hsps are also inducible by TCDD for cytoprotection. Prolonged elevation of Hsps may also participate in carcinogenesis (32).

TABLE 3

List of the 56 Tags with Statistically Significant Differences ($p < 0.01$) between Normal and TCDD-Treated Mouse Liver SAGE Library

| | Tag count | | | | |
|---|---|---|---|---|---|
| *P* | Normal | TCDD | Tag sequence | Unigene | Description |
| <0.00001 | 242 | 493 | ATAATACATA | 142740 | Metallothionein 2 |
| <0.00001 | 93 | 197 | AAAAAAAAAA | | Multiple match |
| <0.00001 | 473 | 642 | ATACTGACAT | 142740 | Metallothionein 2 |
| 0.00001 | 18 | 56 | AGGACTCAGG | 16773 | Serum albumin variant |
| 0.00001 | 2516 | 2837 | AAGACTCAGG | 16773 | Serum albumin variant |
| 0.00006 | 861 | 1038 | AATTTCTTCC | 4516 | Major urinary protein 2 |
| 0.00019 | 0 | 14 | AAGACTCTGG | 16773 | Serum albumin variant |
| 0.00060 | 39 | 76 | GAAAAAAAAA | | Multiple match |
| 0.00075 | 41 | 78 | TTTTCAAAAA | 163 | Beta-2 microglobulin |
| 0.00091 | 58 | 100 | AATTAAAAAC | | Multiple match |
| 0.00110 | 3 | 18 | AATAAAAGTT | | Multiple match |
| 0.00110 | 3 | 18 | AATTTCTCCC | 46221 | Tenomodulin |
| 0.00111 | 5 | 22 | AGTTTCTTCC | | No reliable matches |
| 0.00160 | 0 | 10 | TCTGTCTTTA | 30158 | ESTs, RIKEN cDNA 0710001O03 gene |
| 0.00243 | 17 | 40 | GAATAATAAA | 2944 | Heat shock protein cognate 70 |
| 0.00394 | 20 | 43 | GAGACTCAGG | 16773 | Serum albumin variant |
| 0.00402 | 6 | 21 | TTAAAATATT | 24074 | Solute carrier family (organic anion transporter) member 10 |
| 0.00462 | 2 | 13 | AAGACTAAGG | | No reliable matches |
| 0.00469 | 4 | 17 | AATCTCTTCC | | No reliable matches |
| 0.00469 | 4 | 17 | ATAGACACTA | 15537 | Cytochrome P450, 1a2 |
| 0.00767 | 28 | 52 | GAGTAATACA | 142498 | RIKEN cDNA 0610011L04 gene |
| 0.00769 | 2 | 12 | TAAGAGTTCT | | Multiple match |
| 0.00828 | 0 | 7 | AAGAAAACAT | 22387 | Eukaryotic translation initiation factor 2, subunit 3 |
| 0.00840 | 7 | 21 | AAGTCATTCT | 27448 | Neuropilin |
| 0.00975 | 15 | 33 | TAAAAAAAAA | | Multiple match |
| <0.00001 | 1803 | 1417 | GCTGCCCTCC | 142188 | Delta-like homolog (Drosophila) |
| <0.00001 | 620 | 449 | TGCCCAGGGA | 7010 | Alpha-2-HS-glycoprotein |
| <0.00001 | 679 | 514 | GTGGCTCACA | | Multiple match |
| <0.00001 | 925 | 743 | CATCGCCAGT | 21417 | Apolipoprotein E |
| 0.00009 | 150 | 90 | TCAGGCTGCC | 1776 | Ferritin heavy chain |
| 0.00021 | 639 | 516 | AGTCCACTGG | 16672 | Serine protease inhibitors |
| 0.00067 | 107 | 63 | ATGGTGTTTC | 1090 | Glutathione peroxidase 1 |
| 0.00099 | 213 | 151 | ATGGCACTCA | 23995 | Hepcidin antimicrobial peptide |
| 0.00105 | 20 | 4 | AATTTCACAC | 300 | Carbonic anhydrase 3 |
| 0.00121 | 37 | 14 | GCAGAGTGCG | 1139 | Ribosomal protein S6 |
| 0.00131 | 13 | 1 | TCCACTGTGC | 21840 | EST, RIKEN cDNA 4930542G03 gene |
| 0.00140 | 25 | 7 | AAGCTACAGT | 2044 | Pigment epithelium-derived factor |
| 0.00193 | 164 | 113 | AACGTGCAGG | 3217 | Argininosuccinate synthetase 1 |
| 0.00221 | 60 | 31 | GGTGGTGGTA | 28340 | ESTs |
| 0.00336 | 28 | 10 | GCAGCAATGC | 13000 | Histidine ammonia lyase |
| 0.00381 | 11 | 1 | GACACTCAGG | 5062 | Phosphatidylcholine transfer protein |
| 0.00381 | 11 | 1 | GTGAACCCAA | 26940 | Carbonyl reductase 1 |
| 0.00418 | 233 | 176 | CCCTGGGTTC | | Multiple match |
| 0.00434 | 67 | 38 | GCTCCTGGTG | 24596 | ESTs |
| 0.00442 | 17 | 4 | GCAGAGCAAA | 27361 | Multiple match |
| 0.00459 | 8 | 0 | TGTTCAATCA | 35851 | Sin3-associated polypeptide 18 |
| 0.00459 | 8 | 0 | TTGTGTGACC | 38231 | ESTs |
| 0.00652 | 10 | 1 | ACAACTTCCT | 4140 | GM2 ganglioside activator protein |
| 0.00652 | 10 | 1 | ATGATGGACA | 30049 | Complement component 1, q subcomponent binding protein |
| 0.00709 | 88 | 56 | GTTGCTGACC | 971 | Plasminogen |
| 0.00744 | 14 | 3 | GGAGGCAGAG | 116761 | Carbonic anhydrase 5, mitochondrial |
| 0.00802 | 7 | 0 | GAGTTTCTCT | 90086 | ESTs |
| 0.00802 | 7 | 0 | TAGGGCGGCT | 8356 | Mucolipin 1 |
| 0.00802 | 7 | 0 | TGCCCCAGGT | 141864 | EST, RIKEN cDNA 2810422J05 gene |
| 0.00871 | 24 | 9 | GGCCACGGGA | | Multiple match |
| 0.00910 | 27 | 11 | TGCTTTCTTG | 24267 | ESTs |

*Note.* The numbers of detected tag copies in normal and TCDD-treated mouse liver together with the *p*-value and Unigene ID are shown. Data are classified by up-regulation or down-regulation, and sorted by *p*-value.

TABLE 4

List of Single-Matched and Named Transcripts Responsive to TCDD ($p < 0.05$) with Functional Classification

| Normal | TCDD | Tag | Description |
|---|---|---|---|
| **Signal transduction** | | | |
| 5 | 0 | CTATGGCTTC | RAB11a, member RAS oncogene family |
| 5 | 0 | TACGACGAGT | ral-A protein |
| 5 | 15 | ATGAAATTTC | Interferon-inducible GTPase |
| 13 | 4 | GCTGCTCACT | Insulin-like growth factor binding protein, ALS |
| 16 | 6 | AAGCAGAAGG | Calcium binding protein A11 (calgizzarin) |
| 33 | 53 | TGTGTTATTT | Regucalcin |
| 4 | 0 | CGCTGTACAG | Insulin-like growth factor binding protein 3 |
| 15 | 6 | CCCATTCGGG | S100 calcium binding protein A1 |
| 37 | 22 | GCCTGTCTTC | RAB3D, member RAS oncogene family |
| **Proliferation/cell cycle** | | | |
| 5 | 0 | TATTGTGGCT | Cyclin-dependent kinase inhibitor 1A (P21) |
| **Proteome relation/vesicle trafficking** | | | |
| 6 | 0 | GAGATGCTGG | Proteasome (prosome, macropain) 26S subunit |
| 7 | 1 | GTCCTGCTCT | Proprotein convertase subtilisin/kexin type 6 |
| 4 | 0 | TCCTTTGTAC | Metaxin 2 |
| 0 | 4 | GGTTTTCAAG | Ubiquitin-like 1 |
| 0 | 5 | TGTGTCAACC | Tyrosine 3-monooxygenase activation protein |
| **Transcription factors/regulators** | | | |
| 8 | 0 | TGTTCAATCA | Sin3-associated polypeptide 18 |
| 0 | 7 | AAGAAAACAT | Eukaryotic translation initiation factor 2 |
| 6 | 0 | GATGTGACCA | Eukaryotic translation initiation factor 3 |
| 33 | 16 | ATCAACACCG | Guanine nucleotide binding protein |
| 182 | 140 | AGGCAGACAG | Eukaryotic translation elongation factor 1 |
| 0 | 5 | GGAACAGAAA | Nucleobindin |
| 0 | 5 | TCCCTGGCAT | Heterogeneous nuclear ribonucleoprotein K |
| 9 | 2 | AGTCCTGGAT | High mobility group protein 1 |
| 1 | 7 | ATTGCCCTGC | Heterogeneous nuclear ribonucleoprotein C |
| 33 | 18 | GCCAAGTGGA | Eukaryotic translation elongation factor 2 |
| 15 | 29 | TAAAGCAAAA | Histone gene complex 1 |
| 4 | 0 | AAGAATCAAA | YY1 transcription factor |
| 4 | 0 | TGACTTTTCT | Zinc finger protein 207 |
| 0 | 4 | CCCGCCACCC | Upstream transcription factor 2 |
| 0 | 4 | GAGCAGGAGC | Histone deacetylase 5 |
| 0 | 4 | GTGCCAGGAA | Nuclear RNA export factor 1 homolog |
| 0 | 4 | GTTGTTTGTT | Homeodomain interacting protein kinase 1 |
| 0 | 4 | TACTGTCCTG | RNA polymerase I–3 (16 kDa subunit) |
| 0 | 4 | TGGGGTCTCA | Basic transcription factor 3 |
| **RNA processing/splicing/stability** | | | |
| 37 | 14 | GCAGAGTGCG | Ribosomal protein S6 |
| 35 | 17 | TAGACAGATC | Ribonuclease, RNase A family 4 |
| 24 | 10 | AACAATTTGG | Ribosomal protein L9 |
| 0 | 5 | GTGTATCTTT | Splicing factor, arginine/serine-rich 2 (SC-35) |
| 0 | 5 | TAGTGTGACA | Ribosomal protein S8 |
| 23 | 40 | CACCACCGTT | Ribosomal protein L7a |
| 45 | 28 | CCCCAGCCAG | Ribosomal protein S3 |
| 0 | 5 | GCCAATAGTG | Endothelial monocyte activating polypeptide 2 |
| **Cofactor/chaperone** | | | |
| 504 | 431 | CCCTGAGGGG | Protein that interacts with C kinase 1 |
| 12 | 3 | AAGCTGCTTG | GrpE-like 1, mitochondrial |
| 0 | 4 | CACAGAACCA | Chaperonin subunit 3 (gamma) |
| 0 | 4 | CCCAAGGAGA | Chaperonin subunit 4 (delta) |
| 15 | 6 | GCGTGGCCTG | Enoyl Coenzyme A hydratase, short chain, 1 |
| **Ion pumps/transporter** | | | |
| 11 | 1 | GACACTCAGG | Phosphatidylcholine transfer protein |
| 6 | 21 | TTAAAATATT | Organic anion transporter member 10 |
| 16 | 5 | GCCAGTGCAG | FXYD domain-containing ion transport regulator 1 |
| 14 | 4 | CGTCTGTGGA | ATPase-like vacuolar proton channel |
| 7 | 1 | CTACGGTTGC | ATP-binding cassette, sub-family G (WHITE) |
| **Cell surface** | | | |
| 7 | 21 | AAGTCATTCT | Neuropilin |
| 3 | 18 | AATTTCTCCC | Tenomodulin |
| 6 | 0 | GTGACTCCCA | CD82 antigen |
| 0 | 6 | GTGCACACTC | Poliovirus sensitivity |
| 5 | 0 | GCAGAGTTTT | LDL receptor related protein, associated protein 1 |
| 1 | 7 | GTAGTGGAGC | Integral membrane protein 3 |
| 2 | 9 | GCTGCCCTCG | Natural killer tumor recognition sequence |
| 6 | 15 | GGACCTGTAA | Syndecan 4 |

TABLE 4—*Continued*

| Normal | TCDD | Tag | Description |
|---|---|---|---|
| Growth factors | | | |
| 25 | 7 | AAGCTACAGT | Pigment epithelium-derived factor |
| Enzyme | | | |
| 164 | 113 | AACGTGCAGG | Argininosuccinate synthetase 1 |
| 28 | 10 | GCAGCAATGC | Histidine ammonia lyase |
| 4 | 17 | ATAGACACTA | Cytochrome P450, 1a2 |
| 28 | 51 | CAAAATAAAC | Cytochrome P450, 2d10 |
| 6 | 0 | TGCTGACAAT | Protein phosphatase 1, catalytic subunit |
| 71 | 45 | ATGGTGAGCG | Tryptophan-2,3-dioxygenase |
| 24 | 10 | GGAAGAGGAA | Sialyltransferase 9 |
| 12 | 3 | CAGCTAATGC | Acetyl-Coenzyme A dehydrogenase, long-chain |
| 2 | 10 | ATACTGACGT | Ornithine decarboxylase, structural |
| 40 | 22 | CCTGCCACTG | Ketohexokinase |
| 40 | 22 | GTTGGAGGCT | Plasmin inhibitor alpha 2 |
| 58 | 36 | CAAATAGGTT | Phosphoenolpyruvate carboxykinase 1 |
| 0 | 5 | TTATAGACGG | Stearoyl-Coenzyme A desaturase 1 |
| 93 | 66 | GCCCAGACCT | Sorbitol dehydrogenase 1 |
| 26 | 13 | GCAATCTGAT | Phosphoglycerate kinase 1 |
| 4 | 0 | GTATCCCTGC | Ornithine transcarbamylase |
| 0 | 4 | AGGCGGAGGC | Galactokinase |
| 0 | 4 | TAGCTGTAAC | Lactate dehydrogenase 1, A chain |
| 0 | 4 | TTTTAATGCA | Lysosomal acid lipase 1 |
| Cellular/energy metabolism | | | |
| 11 | 1 | GTGAACCCAA | Carbonyl reductase 1 |
| 20 | 4 | AATTTCACAC | Carbonic anhydrase 3 |
| 14 | 3 | GGAGGCAGAG | Carbonic anhydrase 5 |
| 9 | 23 | TAATAGTAAC | Cytochrome c oxidase, subunit Va |
| 15 | 31 | TACTCATTAT | Cytochrome c oxidase subunit VIIb |
| 31 | 17 | CAGGAGGAGT | Glucose regulated protein, 58 kDa |
| Cell damage, apoptosis, stress | | | |
| 17 | 40 | GAATAATAAA | Heat shock protein cognate 70 |
| 24 | 10 | TGACACAGGA | Cell death-inducing DNA fragmentation factor |
| 10 | 22 | CCTCCCTTTT | Heat shock 10 kDa protein 1 (chaperonin 10) |
| 55 | 35 | TCTCCAGGCG | Clusterin |
| Cytoplasm | | | |
| 321 | 274 | ACATTGGGCG | Fatty acid binding protein 1, liver |
| 18 | 8 | GACACTCTGG | Presenilin 2 |
| 10 | 1 | ACAACTTCCT | GM2 ganglioside activator protein |
| 9 | 1 | TGTTGTGTTT | Peroxisome biogenesis factor 16 |
| 4 | 12 | TAATAGCTAG | Male enhanced antigen 1 |
| 7 | 0 | TAGGGCGGCT | Mucolipin 1 |
| 18 | 8 | AGAGGAGAGA | Gene trap ankyrin repeat |
| Plasma protein | | | |
| 925 | 743 | CATCGCCAGT | Apolipoprotein E |
| 2516 | 2837 | AAGACTCAGG | Serum albumin variant |
| 861 | 1038 | AATTTCTTCC | Major urinary protein |
| 620 | 449 | TGCCCAGGGA | Alpha-2-HS-glycoprotein |
| 150 | 90 | TCAGGCTGCC | Ferritin heavy chain |
| 639 | 516 | AGTCCACTGG | Serine protease inhibitors |
| 41 | 78 | TTTTCAAAAA | Beta-2 microglobulin |
| 213 | 151 | ATGGCACTCA | Hepcidin antimicrobial peptide |
| 10 | 1 | ATGATGGACA | Complement component 1 |
| 88 | 56 | GTTGCTGACC | Plasminogen |
| 203 | 157 | TGGGGCCTCT | Complement component 3 |
| 330 | 273 | AATTCGCGGA | Transthyretin |
| 282 | 230 | GATGAGACAG | Serine protease inhibitor 1-3 |
| 127 | 93 | GAAGAGGGGG | Haptoglobin |
| 118 | 87 | TATTCTGCCC | Alpha-2-glycoprotein 1, zinc |
| 13 | 26 | GTGATCAGAA | Kininogen |
| 335 | 284 | ACCTTGGAAG | Apolipoprotein CI |
| 38 | 22 | GGGATGGACG | Complement component 4 |
| 60 | 85 | AAGAACCAAG | Alpha-2-macroglobulin |
| Detoxification | | | |
| 242 | 493 | ATAATACATA | Metallothionein 1 |
| 473 | 642 | ATACTGACAT | Metallothionein 2 |
| 107 | 63 | ATGGTGTTTC | Glutathione peroxidase 1 |
| Cytoskeleton | | | |
| 21 | 8 | GGCTGGGGGC | Profilin 1 |
| 21 | 9 | CCCTGAGTCC | Melanoma X-actin |
| 24 | 12 | GCACCGAACA | Destrin |
| 4 | 0 | CTCCTGGACA | Gelsolin |
| 0 | 4 | TTGGTGAAGA | Keratin complex 2, basic, gene 1 |
| 4 | 0 | GGGCAAGATG | Prefoldin 2 |

| TCDD - + | Tag Count | | Description |
|---|---|---|---|
|  | 28 | 52 | RIKEN cDNA 0610011L04 |
|  | 8 | 0 | EST, similar to DKFZp564p1263.1 |
|  | 5 | 15 | Interferon-inducible GTPase |
|  | 28 | 10 | Histidine ammonia lyase |
|  | 0 | 3 | CYP 1a1 |
|  | 56 | 44 | GAPDH |

FIG. 2. RT–PCR analysis. RT–PCR analysis of six representative genes differentially expressed is shown with tag count in each SAGE library. The expression levels of selected genes were relative to the abundance of SAGE tags.

*Plasma proteins.* The expression of the genes encoding plasma proteins such as ferritin, apolipoproteins, complements, and plasminogen were downregulated on the whole, suggesting that protein synthesis, which is not urgent, except for acute phase reactions, seems to be reasonably suppressed. Albumin, on the contrary, was induced by TCDD treatment. Albumin is the most representative plasma protein and constitutes almost a half of that in weight. In addition to maintain plasma osmotic pressure, it functions as a carrier protein for many substances. Although it is difficult to conclude precise significance of increase of albumin gene expression, it may work as acute phase response for detoxification.

*Detoxification.* Metallothioneins (MTs) are cysteinrich metal-binding proteins that exert cytoprotective effects against heavy metal toxicity and external stimuli including ionizing or ultraviolet B irradiation. Previous study reported that liver MTs are induced by TCDD treatment, probably to protect against TCDD-generated reactive oxygen species, especially for hydroxyradical, as an antioxidant (33). Our study revealed TCDD induced MTs from 1.27% to over 2.00% of all liver transcriptome mass and also changed the expression of many genes related to oxidative stress. Taken together, TCDD may have stronger impact on oxidative stress than previously considered (34), and TCDD-generated reactive oxygen species would play an important role in TCDD toxicity.

### *Comparison with Previous Studies Using cDNA Array*

Recently, several groups reported gene expression profiles of human hepatoma cell line (HepG2) exposed to TCDD by using cDNA microarray technology, which has been widely used in gene expression profiling (16, 17). Although the results of these studies were partly consistent with our data regarding the genes encoding xenobiotics metabolizing enzymes or plasma proteins, the large proportion was different. Compared with previous studies, we utilized SAGE technology and *in vivo* mouse model. SAGE technology has two major advantages over cDNA microarray technology. First, SAGE technology can detect novel genes. Second, tag count in SAGE analysis directly indicates an expression quantity of each gene in the given samples, therefore the gene expression profile can be compared with other library in a quantitative manner.

It is dubious how exactly hepatocyte cell line cells reflect physiological responses under culture condition. Moreover, HepG2 is derived from hepatoblastoma and have been shown to lose normal metabolic functions (19, 35). Therefore, we considered that usage of HepG2 was insufficient and chose the mouse model administered orally with TCDD, to reflect physiological responses to TCDD. For these reasons, we believe that our study is a faithful description of the *in vivo* gene expression profiles of normal and TCDD-treated mammalian liver.

## CONCLUSION

We have established a mouse liver transcriptome, an important step that enables analyses of gene expression induced in disease states and other biological conditions. The comparison of normal liver and TCDD treated mouse liver revealed 346 differentially expressed transcripts ($p < 0.05$). Most changes were relatively subtle (two- to four-fold). Response to TCDD was substantially more broad and complex than previously reported. Although transcriptome does not necessarily reflect proteome and function, it is definitely beneficial to predict TCDD effects on the liver. We expect that our results will serve as an initial step for the verification of hypotheses designed to connect the gap between the functions of individual TCDD-disregulated genes and the physiological responses to TCDD exposure. Identification of transcripts corresponding to these tags will provide a new clue for clarifying the mechanism of long term influence of TCDD to the liver, novel diagnostic markers, and also enable us to construct an informative microarray system and a high throughput analysis for monitoring the action of numerous environmental pollutants at various time points. In addition, these comprehensive data may be helpful to develop new approach and strategy for prevention and treatment for diseases caused by environmental pollutants.

## ACKNOWLEDGMENT

We are very grateful to Dr. Makoto Haino for helpful discussion.

## REFERENCES


1. Sweeney, M. H., and Mocarelli, P. (2000) *Food Addi. Contam.* **17**, 303–316.
2. Schwarz, M., Buchmann, A., Stinchcombe, S., Kalkuhl, A., and Bock, K. W. (2000) *Toxicol. Lett.* **112-113**, 69–77.
3. IARC (1997) IARC Monographs on the Evaluation of Carcinogenic Risks to Humans, Vol. 69.
4. Hurst, C. H., DeVito, M. J., Setzer, R. W., and Birnbaum, L. S. (2000) *Toxicol. Sci.* **53**, 411–420.
5. Calvart, G. M., Hornung, R. W., Sweeney, M. H., Fingerhut, M. A., and Halperin, W. E. (1992) *JAMA* **267**, 2209–2214.
6. Bertazzi, P. A., Zocchetti, C., Guercilena, S., Consonni, D., Tironi, A., Landi, M. T., and Pesatori, A. C. (1997) *Epidemiology* **8**, 646–652.
7. Lucier, G. W., Tritscher, A., Goldsworthy, T., Foley, J., Clark, G., Goldstein, J., and Maronpot, R. (1991) *Cancer Res.* **51**, 1391–1397.
8. Viluksela, M., Bager, Y., Tuomisto, J. T., Scheu, G., Unkila, M., Pohjanvirta, R., Flodstrom, S., Kosma, V. M., Maki-Paakkanen, J., Vartiainen, T., Klimm, C., Schramm, K. W., Warngard, L., and Tuomisto, J. (2000) *Cancer Res.* **60**, 6911–6920.
9. Abernathy, D. J., Greenlee, W. F., Huband, J. C., and Boreiko, C. J. (1985) *Carcinogenesis* **6**, 651–653.
10. Yang, J.-H., Thraves, P., Dritschio, A., and Rhim, J. S. (1992) *Cancer Res.* **52**, 3478–3482.
11. Okey, A. B., Riddick, D. S., and Harper, P. A. (1994) *Toxicol. Lett.* **70**, 1–22.
12. Safe, S. (2001) *Toxicol. Lett.* **120**, 1–7.
13. Matikainen, T., Perez, G. I., Jurisicova, A., Pru, J. K., Schlezinger, J. J., Ryu, H. Y., Laine, J., Sakai, T., Korsmeyer, S. J., Casper, R. F., Sherr, D. H., and Tilly, J. L. (2001) *Nat. Genet.* **28**, 355–360.
14. Nebert, D. W., Roe, A. L., Dieter, M. Z., Solis, W. A., Yang, Y., and Dalton, T. P. (2000) *Biochem. Pharmacol.* **59**, 65–85.
15. Fox, T. R., Best, L. L., Goldsworthy, S. M., Mills, J. J., and Goldsworthy, T. L. (1993) *Cancer Res.* **53**, 2265–2271.
16. Frueh, F. W., Hayashibara, K. C., Brown, P. O., and Whitelock, J. P., Jr. (2001) *Toxicol. Lett.* **122**, 189–203.
17. Puga, A., Maier, A., and Medvedovic, M. (2000) *Biochem. Pharmacol.* **60**, 1129–1142.
18. Velculescu, V. E., Zhang, L., Vogelstein, B., and Kinzler, K. W. (1995) *Science* **270**, 484–487.
19. Yamashita, T., Hashimoto, S., Kaneko, S., Nagai, S., Toyoda, N., Suzuki, T., Kobayashi, K., and Matsushima, K. (2000) *Biochem. Biophys. Res. Commun.* **269**, 110–116.
20. Hurst, J. L., Payne, C. E., Nevison, C. M., Marie, A. D., Humphries, R. E., Robertson, D. H., Cavaggioni, A., and Beynon, R. J. (2001) *Nature* **414**, 631–634.
21. Cavaggioni, A., and Mucignat-Caretta, C. (2000) *Biochim. Biophys. Acta* **1482**, 218–228.
22. Pigeon, C., Ilyin, G., Courselaud, B., Leroyer, P., Turlin, B., Brissot, P., and Loreal, O. (2001) *J. Biol. Chem.* **276**, 7811–7819.
23. Kerkvliet, N. I. (2002) *Int. Immunopharmacol.* **2**, 277–291.
24. Sagev, N. (2001) *Sci. STKE* **100**, RE11.
25. Hales, C. M., Griner, R., Hobdy-Henderson, K. C., Dorn, M. C., Hardy, D., Kumar, R., Navarre, J., Chan, E. K., Lapierre, L. A., and Goldenring, J. R. (2001) *J. Biol. Chem.* **276**, 39067–39075.
26. Scharf, J. G., Dombrowski, F., and Ramadori, G. (2001) *Mol. Pathol.* **54**, 138–144.
27. Tian, Y., Ke, S., Denison, M. S., Rabson, A. B., and Gallo, M. A. (1999) *J. Biol. Chem.* **274**, 510–515.
28. Ichikawa, T., Itakura, T., and Negishi, M. (1989) *Biochemistry* **28**, 4779–4784.
29. Ohmori, S., Taniguchi, T., Rikihisa, T., Kanakubo, Y., and Kitada, M. (1993) *Xenobiotica* **23**, 419–426.
30. Okino, S. T., and Whitelock, J. P., Jr. (2000) *Vitam. Horm.* **59**, 241–264.
31. Beere, H. M. (2001) *Sci. STKE* **93**, RE1.
32. Garrido, C., Gurbuxani, S., Ravagnan, L., and Kroemer, G. (2001) *Biochem. Biophys. Res. Commun.* **286**, 433–442.
33. Nishimura, N., Miyabara, Y., Suzuki, J. S., Sato, M., Aoki, Y., Satoh, M., Yonemoto, J., and Toyama, C. (2001) *Life Sciences* **69**, 1291–1303.
34. Senft, A. P., Dalton, T. P., Nebert, D. W., Genter, M. B., Hutchinson, R. J., and Shertzer, H. G. (2002) *Toxicol. Appl. Pharmacol.* **178**, 15–21.
35. Okubo, K., Hori, N., Matoba, R., Niiyama, T., Fukushima, A., Kojima, Y., and Matsubara, K. (1992) *Nat. Genet.* **2**, 173–179.

J Gastroenterol 2002; 37:807–814

Journal of Gastroenterology



# Tiny staining spots in liver cirrhosis associated with HCV infection observed by computed tomographic hepatic arteriography: follow-up study

Tomoya Tsuchiyama[1], Shuichi Terasaki[1], Shuichi Kaneko[1], Kyosuke Kaji[1], Kenichi Kobayashi[1], and Osamu Matsui[2]

[1]Department of Gastroenterology, Kanazawa University Hospital, Kanazawa Graduate School of Medical Sciences, 13-1 Takara-machi, Kanazawa 920-8641, Japan
[2]Department of Radiology, Kanazawa University Hospital, Kanazawa Graduate School of Medical Sciences, Kanazawa, Japan

*Background.* It is important to distinguish small lesions with increased arterial perfusion observed by computed tomographic arteriography (CT-A) from hepatocellular carcinoma (HCC). However, the clinical characteristics and prognosis of such lesions have not been clarified. *Methods.* We retrospectively examined 200 patients with cirrhosis related to hepatitis C virus (HCV) infection who had undergone both CT-A and CT arterioportography between 1995 and 1998, and found 80 tiny staining spots (TSS)s, with a diameter of 5–10 mm, by CT-A (35 patients). The mean TSS observation period was 29.0 months. If the major axis was larger than 10 mm and showed a 1.5-fold or more increase, the lesion was regarded as tumor growth (TG). The TSS lesions were divided into two groups according to whether the patient had or did not have HCC. The prognosis of TSS was classified into three groups; HCC-suspected group, nontumor group, and unclassified group, in which TG was negative although transcatheter arterial embolization (TAE) had been performed. *Results.* Of the 40 TSSs in 14 patients without HCC, 2 (5%) were suspected as HCC. Of the 40 TSSs in 21 patients with HCC, 13 (32.5%) were suspected as HCC. There were no significant differences in the size, position, and morphology of TSSs among the three prognostic groups. Of the 7 TSSs with a high signal intensity on T2-weighted magnetic resonance (MR) images, 5 were in the HCC-suspected group. *Conclusions.* We recommend early treatment of TSSs accompanying HCC or showing features of malignancy at the imaging workup.

Key words: tiny staining spot (TSS), CT arteriography (CT-A), hepatocellular carcinoma (HCC), tumor growth, liver cirrhosis

## Introduction

With the clarification of groups of patients at high risk of hepatocellular carcinoma (HCC), screening by computed tomography (CT) has been performed in many patients. CT has been used for the determination of treatment methods and for follow-up observation.[1–4] In the high-risk patients, tiny staining spots (TSS)s were often observed on CT images. With the development from chronic hepatitis to liver cirrhosis, shunts of various sizes are generated in the liver by changes in hemodynamics, such as decreases in portal rami and increases in arterial rami.[5–10] Therefore, it is important to distinguish TSSs from small HCC.[11–17] If TSSs are detected by abdominal ultrasonography, diagnosis is possible by histological examination. However, if lesions cannot be detected by abdominal ultrasonography, diagnosis is difficult. It is necessary to estimate which of these TSSs should be treated, because the treatment for tumor is accompanied by risk and pain for the patient. In this study, we examined all of the increases in microarterial perfusion in patients with liver cirrhosis associated with hepatitis C virus (HCV) infection, including some who had undergone subsegmental or segmental transcatheter arterial embolization (TAE), and we evaluated the percentages of TSSs suspected as HCC and the characteristics of the TSSs.

## Patients and methods

### *Subjects*

We retrospectively examined 200 patients with liver cirrhosis associated with HCV infection who had undergone both helical computed tomographic hepatic arteriography (CT-A) and helical CT arterial portography (CT-AP) at our Radiology Department between January 1995 and December 1998, and found

Received: August 22, 2001 / Accepted: March 8, 2002
*Reprint requests to:* T. Tsuchiyama

80 TSSs, with a diameter of 5mm–10mm, by CT-A (35 patients). We excluded TSSs with a diameter of less than 5mm, taking sampling errors into consideration. Patients who had undergone chemotherapy and who had TSSs in the segment where percutaneous ethanol injection therapy or percutaneous microwave coagulation therapy was performed for the treatment of other hepatic cancer were excluded, taking changes in hemodynamics into consideration. In the 80 TSSs, 40 in 21 patients with liver cirrhosis accompanied by primary HCC and 28 in patients who had undergone TAE were included. The number of TSSs per patient was 1 in 20 patients, 2 in 3 patients, 3 in 6 patients, 4 in 2 patients, and greater than 5 in 4 patients.

*CT-A and CT-AP*

CT-A and CT-AP were performed using an XACTIVE IVR/CT system equipped with an Xvision/SP scanner (Toshiba Medical, Tokyo, Japan). For CT-A, a catheter was indwelled in the celiac artery, while for CT-AP, it was indwelled in the superior mesenteric artery. For CT-A, imaging was started 10s after injection of iodine, at a rate of 1–1.5ml/s, and one image was reconstructed each 2.5–3.5mm, at a table feed speed of 5–7mm/s and at a slice thickness of 5–7mm. For CT-AP, imaging was started 25s after injection of iodine, at a rate of 1–2ml/s, and one image was reconstructed each 3.5mm, at a table feed speed of 7mm/s and at a slice thickness of 7mm.

*TAE*

It was difficult to identify TSS observed by CT-A as HCC or non-HCC, but lesions with enhancement by CT-A and with a defect by CT-AP, excluding those in which an anteroposterior (A-P) shunt was suspected, were treated by subsegmental or segmental TAE if a catheter could be indwelled in the feeding artery, taking the possibility of HCC into consideration (3 liver cirrhosis lesions without primary HCC, 25 liver cirrhosis lesions with primary HCC). TAE was performed by injecting a mixture (1.5–9cc) of epirubicin hydrochloride (20–50mg) and lipiodol and by embolization with gel foam.

*Follow-up and evaluation*

Changes in the sizes of TSSs were examined at an interval of about 6 months (4.2–8.2 months) by dynamic study, using CT and magnetic resonance imaging (MRI). If the major axis of the TSS was larger than 10mm and if the TSS showed a 1.5-fold or more increase, the lesion was regarded as tumor growth (TG).

The prognosis of TSSs was classified into three groups according to the presence or absence of tumor growth (TG) and TAE treatment, namely: HCC-suspected group, TG was positive irrespective of TAE; nontumor group, TAE had not been performed and TG was negative; and unclassified group (UC group), the TSS could not be identified as TG or non-TG because TG may have been negative due to the past TAE treatments. The TSS lesions were divided into two groups (TSSs in patients accompanying HCC and TSSs in patients without HCC) according to the presence or absence of HCC, and the percentages of the HCC-suspected, nontumor, and UC groups were evaluated. In the three groups, the size, position (superficial [within 10mm from the surface of the liver], or central), and morphology (oval type: including circular, wormlike, oval, and dot; wedge type: including wedge; and irregular type, including irregular and others) of the TSSs were examined. The incidences of portal perfusion defects by CT-AP, early enhancement by dynamic CT, low-density areas in the delayed phase, and enhancement by dynamic MRI were also examined.

*Statistical analysis*

Differences between patients with HCC and patients without HCC in the HCC-suspected groups were analyzed for statistical significance using Fisher's direct probability calculation method.

## Results

*Incidence of hepatic cancer in the TSS*

Of the 80 TSSs, 40 were observed in 14 patients without HCC, while the remaining 40 TSSs were observed in 21 patients with HCC. One TSS in a patient with HCC was detected by ultrasonography and classified in the HCC-suspected group because the lesion was histologically diagnosed as highly differentiated HCC. Excluding the 1 TSS examined by hepatic biopsy, 14 TSSs were judged as TG(+) during the follow-up period (6.5–29.5 months; median, 13.1 months). The remaining 65 TSSs, i.e., TG(−), were followed-up over a period of 12.0–57.0 months (median, 32.2 months).

Of the 80 TSSs, 15 (18.8%) were in the HCC-suspected group (which consisted of 1 that was confirmed histologically, 4 of the 51 TSSs without TAE, and 10 of the 28 TSSs treatd by TAE), 47 were in the nontumor group, and 18 were in the UC group (Fig. 1). Of the 40 TSSs in patients without HCC, 1 of the 37 TSSs without TAE and 1 of the 3 TSSs treated by TAE were included in the HCC-suspected group (5.0%) (Fig. 2). Figure 3 shows an example of TSS without TAE in

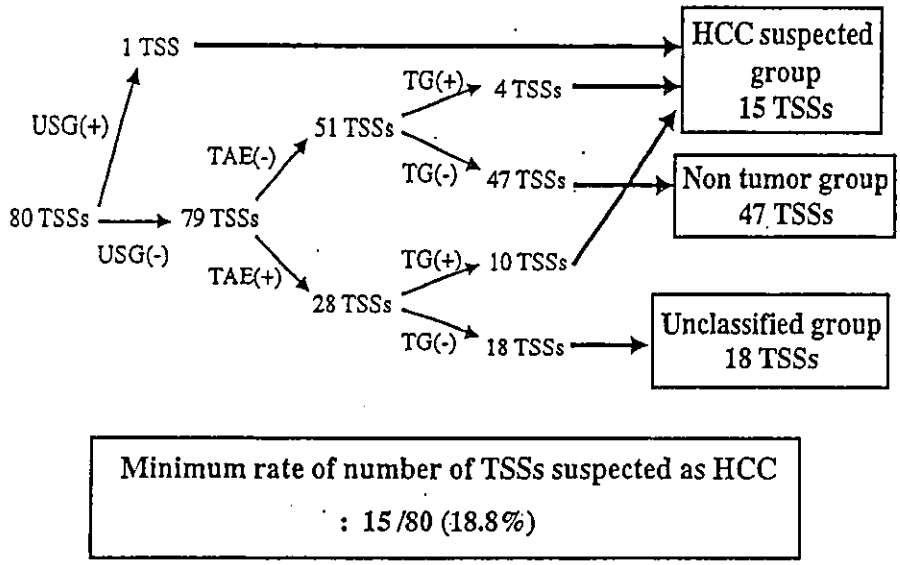


Fig. 1. The prognosis of all tiny staining spots (*TSSs*). *USG(+)*, TSSs detected on ultrasonography; *USG(−)*, TSSs not detected on ultrasonography; *TAE(+)*, TSSs treated by transcatheter arterial embolization (TAE); *TAE(−)*, TSSs not treated by TAE; *TG(+)*, TSSs showing tumor growth; *TG(−)*, TSSs without tumor growth. One TSS was detected by ultrasonography and classified in the hepatocellular carcinoma (*HCC*)-suspected group because the lesion was histologically diagnosed as highly differentiated HCC. Of the 79 remaining TSSs, 14 were classified in the HCC-suspected group; namely, the 4 of 51 TSSs without treatment by TAE, and the 10 of 28 TSSs treated by TAE that showed TG

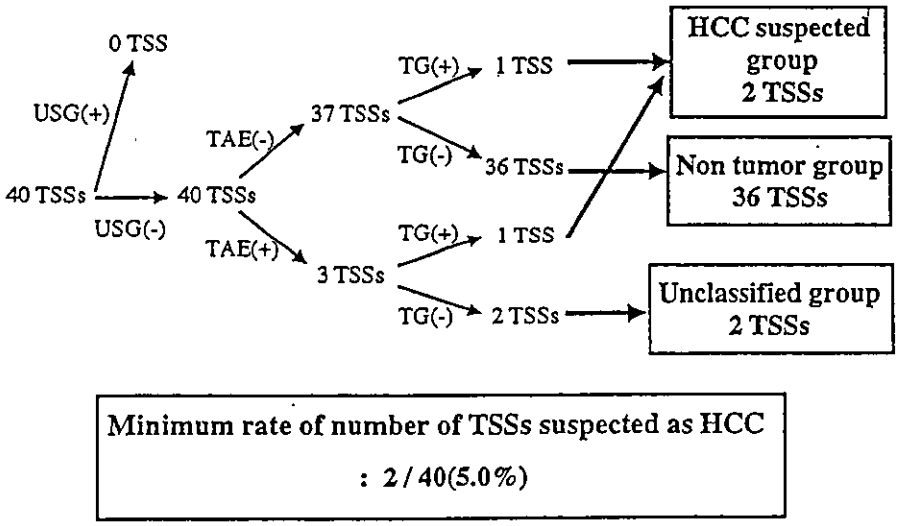


Fig. 2. The prognosis of TSSs in patients without HCC. *USG(+)*, TSSs detected on ultrasonography; *USG(−)*, TSSs not detected on ultrasonography; *TAE(+)*, TSSs treated by TAE; *TAE(−)*, TSSs not treated by TAE; *TG(+)*, TSSs showing tumor growth; *TG(−)*, TSSs without tumor growth. Of the 40 TSSs in patients without HCC, 2 TSSs were classified in the HCC-suspected group; namely, 1 of the 37 TSSs without treatment by TAE and 1 of the 3 TSSs treated by TAE showed TG

the HCC group. Also, of the 40 TSSs in patients with HCC, 1 which was histologically confirmed, 3 of the 14 TSSs without TAE, and 9 of the 25 TSSs treated by TAE were included in the HCC-suspected group (32.5%) (Fig. 4). The possibility of HCC was lower in the TSS group of patients without HCC than in the TSS group of patients with HCC ($P < 0.01$).

Of the 80 TSSs, 52 TSSs had not been treated by TAE and 28 TSSs had been treated by TAE (Fig. 5). In the 52 TSSs without TAE treatment, 37 TSSs were observed in patients without HCC, while the remaining 15 TSSs were observed in patients with HCC. One (2.7%) of the 37 TSSs in patients without HCC and 4 (26.7%) of the 15 TSSs in patients with HCC were included in the HCC-suspected group (Fig. 5). There was a significant difference between the two groups (i.e., those with and without HCC) ($P < 0.05$).

*TSS images and hepatic cancer*

There were no differences in the position, size, and morphology of TSSs observed by CT-A among the HCC-suspected, nontumor, and UC groups (Table 1). The incidence of portal perfusion defects observed by CT-AP was 100% in the HCC-suspected group, 60% in the non-tumor group, and 78% in the UC group, and there was no difference in the morphology of defect among the three groups (Table 2). On the other hand,

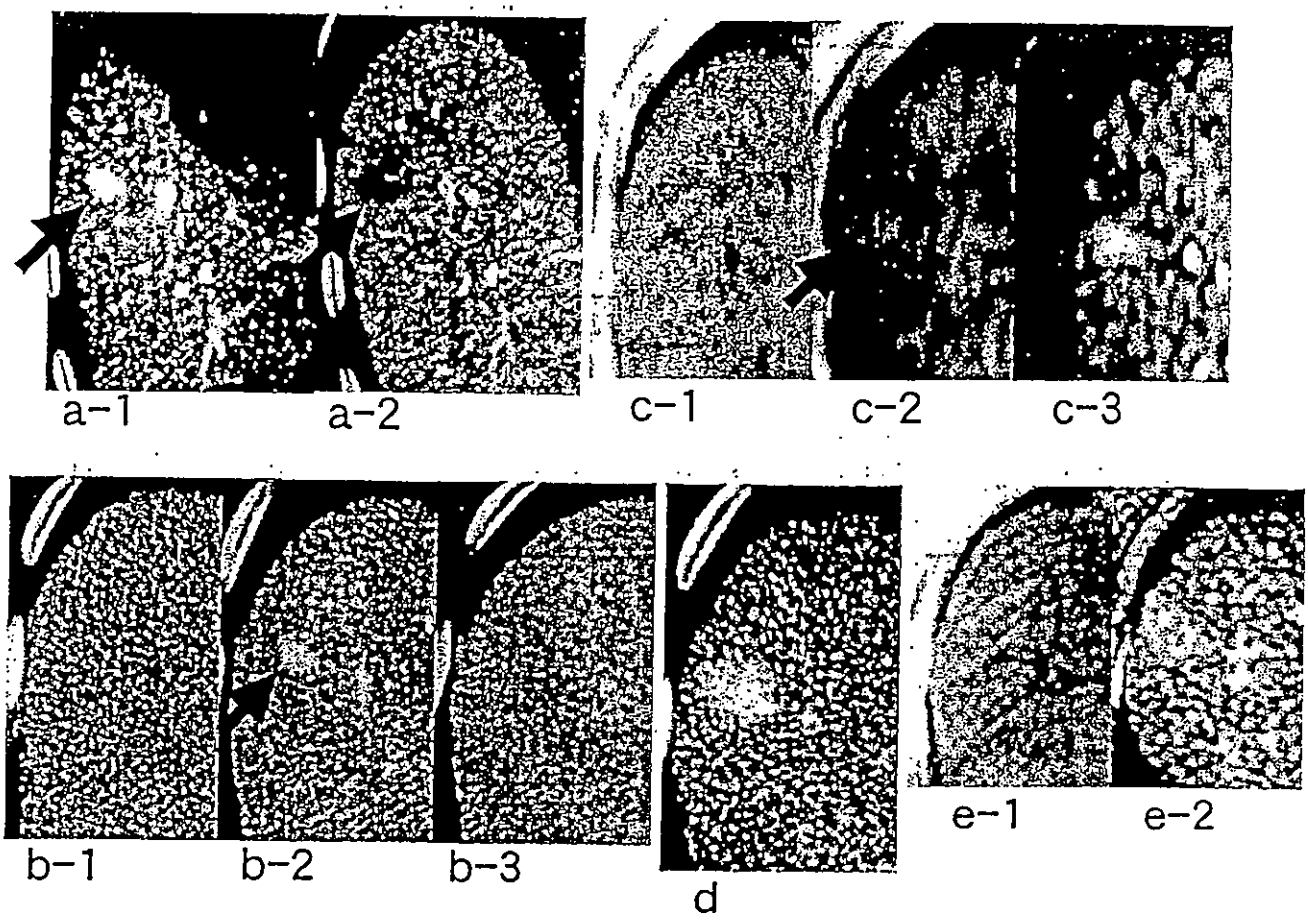


Fig. 3a–e. Example of TSS without TAE treatment and with tumor growth in a patient without HCC. **a-1**, Computed tomographic arteriography (CT-A); **a-2**, CT-arterioportography (AP); **b-1**, precontrast CT; **b-2**, early-phase CT; **b-3**, delayed-phase CT; **c-1**, T1-weighted (wt) magnetic resonance imaging (MRI); **c-2**, T2-wt MRI; and **c-3**, early phase of MRI obtained when TSS was detected. **d** Early-phase CT; **e-1**, T1-wt MRI; and **e-2**, T2-wt MRI obtained when tumor growth was noted. The TSS shown by the *arrow* in **a-1** and the *arrow* in **c-2** was 0.8 cm in diameter and located inside. At first, the TSS showed a high signal on CT-A, low signal on CT-AP, high signal on dynamic CT obtained in the arterial dominant phase, slightly high signal on T2-wt MRI, and high signal in the early phase of dynamic MRI. Tumor growth was noted after 19 months (diameter, 1.2 cm)

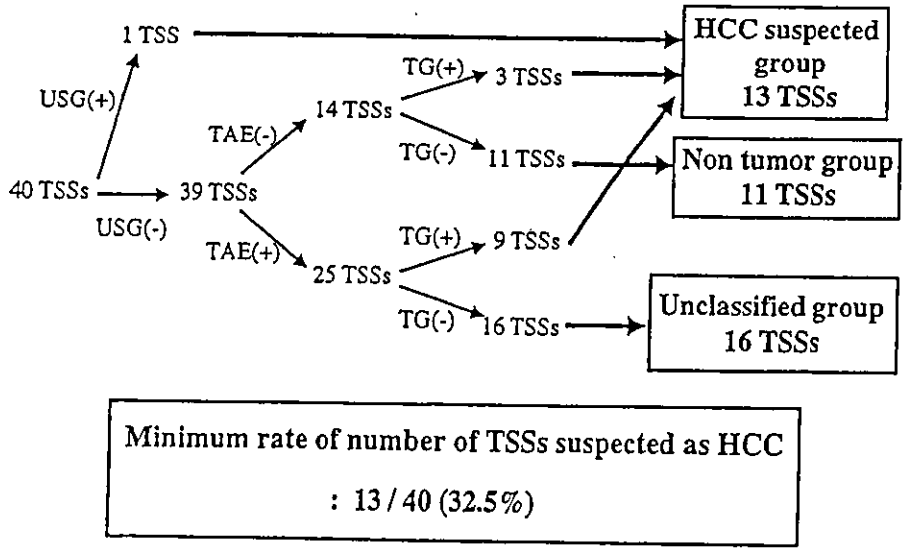


Fig. 4. The prognosis of TSSs in patients with HCC. *USG(+)*, TSSs detected on ultrasonography; *USG(−)*, TSSs not detected on ultrasonography; *TAE(+)*, TSSs treated by TAE; *TAE(−)*, TSSs not treated by TAE; *TG(+)*, TSSs showing tumor growth; *TG(−)*, TSSs without tumor growth. One TSS was detected by ultrasonography and classified in the HCC-suspected group because the lesion was histologically diagnosed as highly differentiated HCC. Of the 39 remaining TSSs, 12 TSSs were classified in the HCC-suspected group; namely, 3 of the 14 TSSs without treatment by TAE and 9 of the 25 TSSs treated by TAE showed TG

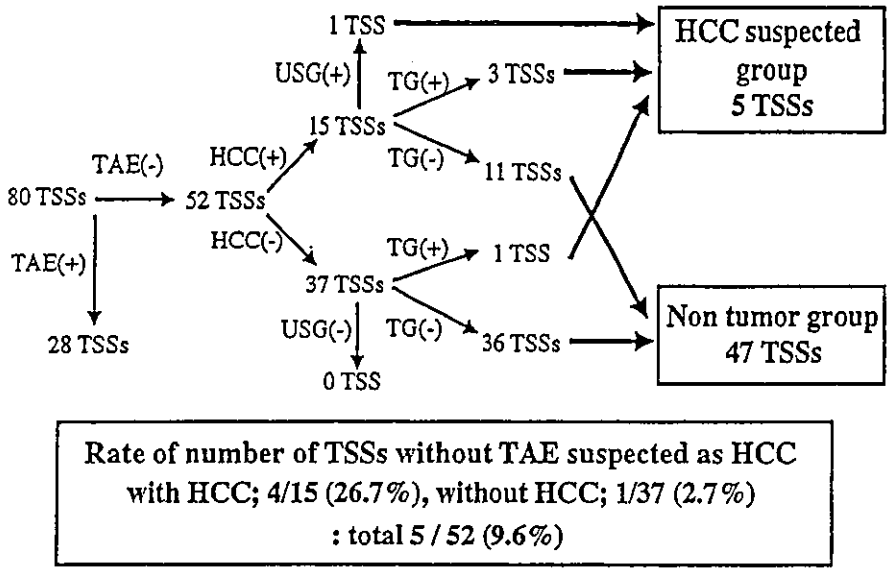


Fig. 5. The prognosis of TSSs without TAE treatment. *TAE(+)*, TSSs treated by TAE; *TAE(−)*, TSSs not treated by TAE; *HCC(+)*, TSSs in patients with HCC; *HCC(−)*, TSSs in patients without HCC; *USG(+)*, TSSs detected on ultrasonography; *USG(−)*, TSSs not detected on ultrasonography; *TG(+)*, TSSs showing tumor growth; *TG(−)*, TSSs without tumor growth. Of the 80 TSSs, 52 TSSs had not been treated by TAE. Of these 52 TSSs, 15 were in patients with HCC and 37 were in patients without HCC. Of the 15 TSSs in HCC(+), 4 were in the HCC-suspected group and 11 were in the nontumor group. Similarly, of the 37 TSSs in HCC(−), 1 was in the HCC-suspected group and 36 were in the nontumor group

**Table 1.** The size, site, and shape of TSSs on CT-A

| | | Site | | Shape | | |
|---|---|---|---|---|---|---|
| | Size (mm) | Surface | Inside | Oval | Wedge | Irregular |
| HCC-suspected group ($n$ = 15) | 7.2 ± 1.7 | 10 (67%) | 5 (33%) | 11 (74%) | 2 (13%) | 2 (13%) |
| Nontumor group ($n$ = 47) | 7.4 ± 1.9 | 31 (66%) | 16 (34%) | 26 (55%) | 15 (32%) | 5 (13%) |
| Unclassified group ($n$ = 18) | 7.2 ± 2.0 | 11 (61%) | 7 (39%) | 13 (72%) | 3 (17%) | 2 (11%) |

TSS, Tiny staining spot; CT-A, computed tomographic hepatic arteriography; HCC, hepatocellular carcinoma

**Table 2.** Portal perfusion and shape of TSSs on CT-AP

| | Portal perfusion | | Shape | | |
|---|---|---|---|---|---|
| | Defect | No defect | Oval | Wedge | Irregular |
| HCC-suspected group ($n$ = 15) | 15 (100%) | 0 (0%) | 10 (67%) | 3 (20%) | 2 (13%) |
| Nontumor group ($n$ = 47) | 28 (60%) | 19 (40%) | 14 (50%) | 12 (43%) | 2 (7%) |
| Unclassified group ($n$ = 18) | 14 (78%) | 4 (22%) | 11 (79%) | 2 (14%) | 1 (7%) |

TSS, Tiny staining spot; CT-A, computed tomographic hepatic arteriography; HCC, hepatocellular carcinoma; CT-AP, computed tomographic arterioportography

the number of TSSs without defect of portal perfusion was 0 in the HCC-suspected group, 19 in the nontumor group, and 4 in the UC group. There were no differences in the incidences of early enhancement by dynamic CT and low-density areas in the delayed phase between the HCC-suspected and nontumor groups (Table 3). Of the 15 TSSs in the HCC-suspected group, 5 were enhanced on the T1- and T2-weighted MR images, and all 5 showed a high signal intensity on the T2-weighted MR images (Table 4). On the other hand, the 7 TSSs showing a high signal intensity on the T2-weighted MR images consisted of 5 in the HCC-suspected group, 1 in the nontumor group, and 1 in the UC group. In addition, of the 43 TSSs in the nontumor group, the one that showed a high signal intensity on the T2-weighted MR image was identical to the one imaged in the CT delayed phase.

## Discussion

It has been reported that CT-A is useful for the identification of portal perfusion defects observed by CT-AP.[5-13] In advanced liver cirrhosis with portal perfusion disorder caused by shunts, tumor embolization, and embolism, there are risks of overlooking tumors with afferent blood vessels due to irregular enhancement by CT-AP, but tumors can be often detected by CT-A.[14-17] Kanematsu et al.[18,19] reported that the sensitivity of imaging of hepatic tumors by the combination of CT-A and CT-AP was not clearly better than that by CT-AP alone, because variously shaped nonpathologic tiny staining spots (TSSs) were observed on the surface of the liver by CT-A, but the specificity was higher with the combination of CT-A and CT-AP. However, with the elevation of the sensitivity of CT, TSSs that could represent small hepatic cancer, shunts in the liver, hepatic hemangioma, and focal nodular hyperplasia (FNH) have become detectable, and the distinction between these possibilities is difficult. In this study, we examined these TSSs comprehensively and evaluated the disease courses for the first time.

One of the important findings in this study was that TSSs in patients without primary HCC were unlikely to be HCC, and TSSs in patients with primary HCC had a comparatively high possibility of being HCC. It was reported that HCC recurrence was caused by multicentric recurrence and intrahepatic metastasis, as well as local recurrence, and was observed in about 30% of patients after 1 year.[20] Our results are consistent with this report, in that the percentage of TSSs showing TG(+) was higher in patients with primary HCC than that in patients without primary HCC.

It was reported that nonpathologic TSSs were often oval or wedge-shaped.[18,19] In our results, the percentage of wedge-shaped lesions was 32% in the nontumor group, which was slightly higher than that in the other groups. Non-pathologic TSSs were often observed on the surface of the liver, while anatomical variations of arterial perfusion into the liver (around the gallbladder solum, shunts between veins and sinusoids around the falciform ligament of the liver, pressed perfusion abnormality in the regions adjacent to the right ribs and surrounding organs and in other regions, small shunts in the peripheral parenchyma of the liver, and perfusion defect caused by the lack of portal perfusion) were reported.[14-17] However, no differences in portal perfusion according to TSS groups were observed in the present study. The portal perfusion defect observed by CT-AP was not specific to the HCC-suspected group, but the possibility of HCC in TSSs without portal perfusion defect was considered low. These results indicated that 4 TSSs without portal perfusion defect in the UC group might have been nontumor. Overt HCC is generally imaged with a high signal intensity on T2-weighted images.[21] In the present study, all TSSs imaged by MRI in

Table 3. Detection of TSSs on dynamic CT

| | Enhancement in early phase | Low-density area in delayed phase |
|---|---|---|
| HCC-suspected group ($n$ = 15) | 5 (33%) | 1 (7%) |
| Nontumor group ($n$ = 47) | 19 (40%) | 1 (2%) |
| Unclassified group ($n$ = 18) | 10 (56%) | 6 (33%) |

TSS, Tiny staining spot; CT, computed tomography; HCC, hepatocellular carcinoma

Table 4. Detection of TSSs on dynamic MRI

| | Enhancement in early phase | Abnormal intensity (T1 wi or T2 wi) | → | T2wi High intensity |
|---|---|---|---|---|
| HCC-suspected group | 5/12 (42%) | 5/12 (42%) | → | 5/5 (100%) |
| Nontumor group | 20/40 (50%) | 4/43 (9%) | → | 1/4 (25%) |
| Unclassified group | 4/17 (24%) | 3/17 (18%) | → | 1/3 (33%) |

TSS, Tiny staining spot; MRI, magnetic resonance imaging; HCC, hepatocellular carcinoma; wi, weighted image

the HCC-suspected group showed a high signal intensity on the T2-weighted images. Of the 4 TSSs imaged by MRI in the nontumor group, 3, apart from the one node imaged in the CT delayed phase, showed a low signal intensity on the T2-weighted images. These three nodes showed a low-to-iso signal intensity on the T1-weighted images, suggesting that regenerated nodes, coagulated necrosis, or blood vessels were imaged. These results indicated that the one node imaged with a high signal intensity on the MR T2-weighted image in the UC group might have been HCC.

Because the growth rate of HCC varies widely, it is difficult to unambiguously define TG. In this study, if the axis of TSS showed a 1.5-fold or more increase, the lesion was regarded as TG, taking measuring errors into consideration. It was reported that the tumor volume doubling time of HCC showing enhancement was less than 3 months,[22] indicating that the growth of HCC is rapid. Therefore, in the present study, the tumors that did not show growth during the observation period (12 months at the shortest; mean, 32.2 months) were classified in the nontumor group. Solid tumors, except for HCC, such as FNH and adenoma, can show clear growth and enhancement, but these diseases are very rare in patients with chronic viral diseases in the liver. Although there is a possibility that TSSs caused by A-P shunt also enlarge during the follow-up period, it is very difficult to distinguish such TSSs from HCC, except by histological methods, and it is ethically difficult to follow-up such TSSs without treatment. Therefore, it was considered adequate that the TSSs of TG(+) were highly suspected as HCC in this study. The growth of some hemangioma lesions is slow, but there were no lesions in the HCC-suspected group showing a high signal intensity on the T2-weighted images after growth, which is characteristic of hemangioma. Because HCC with a high arterial vascularity histologically shows a low degree of differentiation[23,24] and often shows metastasis in the liver,[25] treatment is usually started in the early stages. Therefore, when the axis of TSS showed a 1.5-fold increase, continuation of observation without treatment could be an ethical problem.

In conclusion, because the probability of HCC was suspected to be high if enhancement by CT-A was observed in liver cirrhosis accompanying primary HCC, early treatment or cautious follow-up observation were recommend. The probability of HCC in nodes showing a high signal intensity on T2-weighted MR images was suspected to be high, while that of HCC in nodes without portal perfusion defects was suspected to be low. In this study, we evaluated TSS observed by CT-A, and the results will be useful for the determination of treatment methods for nodes showing microenhancement by CT.

## References


1. Patrick CF, William MM. Patterns of contrast enhancement of benign and malignant hepatic neoplasms during bolus dynamic and delayed CT. Radiology 1986;160:613–8.
2. Nelson RC, Chezmar JL, Sugarbaker PH, Bernardino ME. Hepatic tumors: comparison of CT during arterial portography, delayed CT, and MR imaging for preoperative evaluation. Radiology 1989;172:27–34.
3. Ueda K, Matsui O, Kawamori Y, Nakanuma Y, Kadoya M, Yoshikawa J, et al. Hypervascular hepatocellular carcinoma: evaluation of hemodynamics with dynamic CT during hepatic arteriography. Radiology 1983;146:721–7.
4. Nelson RC, Thompson GH, Chezmar JL, Harned RK II, Fernandez MP. CT during arterial portography: diagnostic pitfalls. Radiographics 1992;12:705–18.
5. Chezmar JL, Bernardino ME, Kaufman SH, Nelson RC. Combined CT arterial portography and CT hepatic angiography for evaluation of the hepatic resection candidate. Radiology 1993; 189:407–10.
6. Saitoh S, Ikeda K, Koida I, Tsubota A, Arase Y, Chayama K, et al. Small hepatocellular carcinoma: evaluation of portal blood flow with CT during arterial portography performed with balloon occlusion of hepatic artery. Radiology 1994;193:67–70.
7. Matsui O, Kadoya M, Kameyama T, Yoshikawa J, Takashima T, Nakanuma Y, et al. Benign and malignant nodules in cirrhotic livers: distinction based on blood supply. Radiology 1991;178:493–7.
8. Paulson EK, Baker ME, Hilleren DJ, Jones WP, Knelson MH, Nadel SN, et al. CT arterial portography: causes of technical failure and variable liver enhancement. AJR AM J Roentgenol 1992;159:745–9.
9. Yamagami T, Arai Y, Matsueda K, Inaba Y, Sueyoshi S, Takeuchi Y. The cause of nontumorous defects of portal perfusion in the hepatic hilum revealed by CT during arterial portiography. AJR Am J Roentgenol 1999;172:397–402.
10. Pando A, Wallace S, Bernardino ME, Lindell MJ. Computed tomographic arteriography of the liver. Radiology 1979;130:697–701.
11. Freeny PC, Marks WM. Hepatic perfusion abnormalities during CT angiography: detection and interpretation. Radiology 1986; 159:685–91.
12. Marchal G, Tshibwabwa-Tunda E, Verveken E, Van Roost W, Van Steenbergen W, Baert A, et al. "Skip areas" in hepatic steatosis: a sonographic-angiographic study. Gastrointest Radiol 1986;11:151–7.
13. Itai Y, Moss AA, Goldberg HI. Transient attenuation difference of lobar or segmental distribution detected by dynamic computed tomography. Radiology 1982;143:719–26.
14. Fernandez MP, Bernardo ME. Hepatic pseudolesion: appearance of focal low attenuation in the medial segment of the left lobe at CT arterial portography. Radiology 1991;181:809–12.
15. Kanematsu M, Kondo H, Enya M, Yokoyama R, Hoshi H. Nondiseased portal perfusion defects adjacent to the right ribs shown on helical CT during arterial portography. AJR Am J Roentgenol 1998;171:445–8.
16. Matsui O, Takashima T, Kadoya M, Konishi H, Kawamura I, Hirose J, et al. Staining in the liver surrounding gallbladder fossa on hepatic arteriography caused by increased cystic venous drainage. Gastrointest Radiol 1987;12:307–12.
17. Matsui O, Takashima S, Kadoya M, Yoshikawa J, Gabata T, Takashima T, et al. Pseudolesion in segument IV of the liver at CT during arterial portography: correlation with aberrant gastric venous drainage. Radiology 1994;193:31–5.
18. Kanematsu M, Hoshi H, Imaeda T, Yamazaki Y, Mizuno S, Manabe T, et al. Nonpathological focal enhancements on spiral CT hepatic angiography. Abdom Imaging 1997;22:55–9.
19. Kanematsu M, Hoshi H, Imaeda T, Murakami T, Inaba Y, Yokoyama R, et al. Detection and characterization of hepatic

tumor: value of combined helical CT hepatic arteriography and CT during arterial portography. AJR Am J Roentgenol 1997; 168:1193–8.
20. Hino O, Kitagawa T, Sugano H. Relationship between serum and histochemical markers for hepatitis B virus and rate of viral integration in hepatocellular carcinomas in Japan. Int J Cancer 1985;35:5–10.
21. Kadoya M, Matsui O, Takashima T, Nonomura A. Hepatocellular carcinoma: correlation of MR imaging and histopathologic findings. Radiology 1992;183:819–25.
22. Tochio H, Tomita S, Kudo M, Mimura J, Hamada M, Minowa K, et al. Growth speed of hepatocellular carcinoma: relationship with arterial vascularity evaluated by US angiography (in Japanese with English abstract). Acta Hepatol Japonica (Jpn Soc Hepatol) 1992;24:758–65.
23. Hayashi M, Matsui O, Ueda K, Kawamori Y, Kadoya M, Yoshikawa J, et al. Correlation between the blood supply and grade of malignancy of hepatocellular nodules associated with liver cirrhosis: evaluation CT during intraarterial injection of contrast medium. AJR Am J Roentgenol 1999;172:969–76.
24. Nakashima Y, Nakashima O, Hsia CC, Kojiro M, Tabor E. Vascularization of small hepatocellular carcinomas: correlation with differentiation. Liver 1999;19:12–8.
25. Oda T, Tsuda H, Scarpa A, Sakamoto M, Hirohashi S. *p53* gene mutation spectrum in hepatocellular carcinoma. Cancer Res 1992; 52:6358–64.

*Brief Definitive Report*

# Prevention of Hepatocellular Carcinoma Development Associated with Chronic Hepatitis by Anti-Fas Ligand Antibody Therapy

Yasunari Nakamoto,[1,2] Shuichi Kaneko,[1] Hong Fan,[2] Takashi Momoi,[3] Hiroko Tsutsui,[4] Kenji Nakanishi,[4] Kenichi Kobayashi,[1] and Takashi Suda[2]

[1]*Department of Gastroenterology, Graduate School of Medicine, and* [2]*Center for the Development of Molecular Target Drugs, Cancer Research Institute, Kanazawa University, Kanazawa, Ishikawa 920-0934, Japan*

[3]*Division of Development and Differentiation, National Institute of Neuroscience, National Center of Neurology and Psychiatry, Kodaira, Tokyo 187-8502, Japan*

[4]*Department of Immunology and Medical Zoology, Hyogo College of Medicine, Nishinomiya, Hyogo 663-8501, Japan*

## Abstract

A persistent immune response to hepatitis viruses is a well-recognized risk factor for hepatocellular carcinoma. However, the molecular and cellular basis for the procarcinogenic potential of the immune response is not well defined. Here, using a unique animal model of chronic hepatitis that induces hepatocellular carcinogenesis, we demonstrate that neutralization of the activity of Fas ligand prevented hepatocyte apoptosis, proliferation, liver inflammation, and the eventual development of hepatocellular carcinoma. The results indicate that Fas ligand is involved not only in direct hepatocyte killing but also in the process of inflammation and hepatocellular carcinogenesis in chronic hepatitis. This is the first demonstration that amelioration of chronic inflammation by some treatment actually caused reduction of cancer development.

Key words: disease model • apoptosis • inflammation • cytotoxic T lymphocytes • cancer

## Introduction

Hepatitis B virus (HBV) is one of the most common pathogens; more than 350 million people are estimated to be chronically infected with it, worldwide. Hepatitis C virus is also a widespread pathogen, which has a worldwide seroprevalence of ~1%. These two pathogens are the major cause of chronic liver inflammation, leading to hepatocellular carcinoma (HCC).

CTLs have been implicated in both the eradication of viruses and liver injury in viral hepatitis patients (1, 2). It has been previously demonstrated that the transfusion of a highly active $CD8^+$ CTL clone that is specific for the hepatitis B surface antigen (HBsAg) induces lethal fulminant hepatitis in transgenic mice that express the HBsAg specifically in the liver (3). We further demonstrated that Fas ligand (FasL), one of the major cytocidal molecules produced by CTLs (4, 5) plays an important role in the pathogenesis of this disease, and that the administration of soluble Fas (Fas–Fc fusion protein that can neutralize FasL) rescues mice from the fatal disease (6, 7). On the other hand, it is generally believed that apoptosis is a mechanism to prevent carcinogenesis. Therefore, it was possible that treatment of hepatitis patients with a FasL-neutralizing agent might increase the risk of hepatic cancer. However, we have not been able to investigate this possibility, because the CTL clone induces neither chronic liver diseases nor HCC.

HCC occurs after many years of chronic hepatitis. The cycles of liver cell destruction and regeneration by repetitive inflammation are thought to set up the mitogenic and mutagenic environment leading to HCC development (8–11). In an effort to clarify the carcinogenic potential of persistent inflammation, one of us (Y. Nakamoto) recently developed a unique animal model of chronic hepatitis that leads to HCC (12). In this model, an investigator transfuses HBsAg-primed splenocytes from wild-type mice into the aforementioned HBsAg transgenic mice. Immune responses against HBsAg are essentially involved in the development of liver diseases including HCC, because the transgenic mice are healthy unless primed splenocytes are transfused. Using this model, we have investigated how treatment by an anti-FasL neutralizing antibody affects in the progression of chronic hepatitis and the development of HCC.

Address correspondence to Takashi Suda, Center for the Development of Molecular Target Drugs, Cancer Research Institute, Kanazawa University, 13-1 Takaramachi, Kanazawa, Ishikawa 920-0934, Japan. Phone: 81-76-265-2736; Fax: 81-76-234-4525; E-mail: sudat@kenroku.kanazawa-u.ac.jp

 J. Exp. Med. © The Rockefeller University Press • 0022-1007/2002/10/1105/7 $5.00
Volume 196, Number 8, October 21, 2002 1105–1111
http://www.jem.org/cgi/doi/10.1084/jem.20020633

## Materials and Methods

*HBV Transgenic Mice.* HBsAg transgenic mouse lineage 107–5D (official designation Tg[Alb-1,HBV]Bri66; inbred B10D2, H-$2^d$) was provided by Dr. F.V. Chisari (The Scripps Research Institute, La Jolla, CA; reference 13). Lineage 107–5D contains the entire HBV envelope-coding region (subtype ayw) under the constitutive transcriptional control of the mouse albumin promoter (13). These mice express the HBV small, middle, and large envelope proteins in their hepatocytes (13). They are immunologically tolerant to HBsAg at the T cell level (14) and they display no evidence of liver disease during their lifetime, without the adoptive transfer of HBsAg-specific CTLs (13, 15). There is no X-RNA or X-protein expression detectable in the livers of these animals (unpublished data).

*Disease Model.* The animal model of chronic hepatitis was generated as described previously (12). Briefly, male HBsAg transgenic mice were thymectomized, irradiated (900 cGy), and their hemopoietic system was reconstituted with bone marrow cells from syngeneic nontransgenic B10D2 (H-$2^d$) mice. 1 wk after the bone marrow transfer, the animals received the indicated numbers of splenocytes from nontransgenic B10D2 (H-$2^d$) mice that were infected intraperitoneally with a recombinant vaccinia virus expressing HBsAg (HBs-vac) 3 wk before the splenocyte transfer (15).

*Preparation and Administration of Anti-FasL mAb.* The anti-mouse FasL mAb (FLIM58) was produced and purified using a protein A column as described previously (16). 2 ng of anti-FasL mAb used in this study completely neutralized the cytotoxicity of 5 units of recombinant mouse FasL. 500 μg of the anti-mouse FasL mAb or control hamster IgG (ICN Biomedicals), or PBS alone was administered intraperitoneally or subcutaneously daily for seven consecutive days (day 0 to 6), and 200 μg anti-mouse FasL mAb, control IgG, or PBS alone was injected every other day between the second and fourth week (day 7 to 28) after adoptive transfer of HBsAg-primed nontransgenic mouse splenocytes.

*Measurement of Serum Alanine Aminotransferase Activity and IL-18.* Serum alanine aminotransferase (ALT) activity was determined as described previously (11). Serum IL-18 was measured by ELISA kits provided by Hayashibara (Okayama, Japan), as reported previously (17).

*Immunohistochemical Analysis.* Tissue samples were fixed in buffered zinc formalin (Anatech Ltd.), embedded in paraffin, sectioned (at 3 μm), and stained with hematoxylin and eosin as described previously (12). Some of the paraffin sections were treated with anti-proliferating cell nuclear antigen (PCNA) primary solution (Dako) at a 1:10 dilution, followed by biotin-conjugated secondary antibody (Vector Laboratories). $PCNA^+$ cells were then visualized using a VECTASTAIN ABC Standard Kit (Vector Laboratories), and the tissue sections were counterstained with hematoxylin before mounting. Liver tissues were also embedded in OCT compound (Sakura Finetek) and snap-frozen in liquid nitrogen. Cryostat sections of frozen tissues were fixed in 4% paraformaldehyde overnight at 4°C. After blocking biotin, the tissue sections were incubated with rabbit anti-mouse active caspase-3 antibodies (18) at a 1:400 dilution for 30 min at room temperature, followed by biotin-conjugated goat anti-rabbit IgG secondary antibodies (Vector Laboratories). The reaction was visualized in the same way as the PCNA staining described above. The TdT-mediated digoxigenin-dUTP nick-end labeling (TUNEL) analysis was performed on serial liver sections according to the manufacturer's instructions (Roche).

*Detection of HBV-specific $CD8^+$ T Lymphocytes.* Intrahepatic lymphocytes (IHLs) were stained with Cy-Chrome–conjugated anti–mouse CD8 mAb (53–6.7; BD Biosciences) in round-bottom 96-well plates. Otherwise, IHLs were cultured for 5 h at 37°C in complete RPMI medium containing 10% FBS in the presence or absence of $10^{-7}$ M of the peptide representing residues 28–39 of HBsAg (IPQSLDSWWTSL) or the lymphocytic choriomeningitis virus nucleoprotein (LCMV NP) peptide (PQASGVYML). Brefeldin A (Sigma-Aldrich), which inhibits exocytosis of the cytokines, was added at a final concentration 2 μg/ml. Subsequently, the cells were stained with Cy-Chrome-anti–mouse CD8 mAb. They were then permeabilized using the Cytofix/Cytoperm kit (BD Biosciences) and stained with allophycocyanin (APC)-conjugated rat mAb specific for mouse IFN-γ (XMG1.2) or its isotype control Ab (rat $IgG_1$; BD Biosciences). Cells were resuspended in PBS containing 2% formaldehyde, and analyzed on a FACSCalibur™ flow cytometer (50,000–300,000 gated events acquired per sample) using CELLQuest™ software (Becton Dickinson).

## Results

*Anti-FasL mAb Diminished Not Only Hepatocyte Apoptosis but Also Inflammation and Hepatocyte Proliferation.* As we reported previously (12), transplantation of total splenocytes from HBsAg-primed mice into HBsAg-transgenic mice induced relatively slow and prolonged acute-phase liver injury, compared with CTL clone-induced hepatitis (3) or other animal models of acute hepatitis. The liver injury peaked 1 wk after the transplantation and gradually resolved thereafter, as revealed by the change in the serum ALT level (Fig. 1 A). Consistent with this, on day 7 we observed strong activation of caspase-3 and DNA degradation (shown by TUNEL), indicating massive hepatocyte apoptosis that occurred along the edge of inflammatory infiltration (Fig. 1 B). Interestingly, the number of active caspase-$3^+$ cells peaked in the second week and was much greater than the number of $TUNEL^+$ cells at the same time point (Fig. 1 C). This observation may suggest that some hepatocytes became relatively resistant to caspase-3 activation after prolonged inflammation.

Because we previously demonstrated that the Fas–Fc fusion protein that can neutralize FasL has therapeutic potential against the fulminant hepatitis induced by a $CD8^+$ CTL clone (6), we thought that treatment with an anti-FasL neutralizing antibody might suppress the activity of hepatitis in this model. As we expected, administration of anti-FasL mAb intraperitoneally and subcutaneously decreased the mean ALT level at day 7 to ~30% and 60%, respectively, of that in the mice that received PBS (Fig. 1 A). Therefore, in the following experiments, we administered mAb intraperitoneally. In accordance with the reduction in serum ALT levels, both caspase-3 activation and DNA degradation in hepatocytes 1 to 4 wk after the splenocyte transfer were greatly diminished by the anti-FasL mAb treatment (Fig. 1, B and C). The anti-FasL mAb treatment not only inhibited hepatocyte apoptosis but also reduced the size and number of inflammatory foci in the liver (Fig. 1 B, and data not depicted). We investigated serum IL-18 levels, because we previously discovered that FasL induces

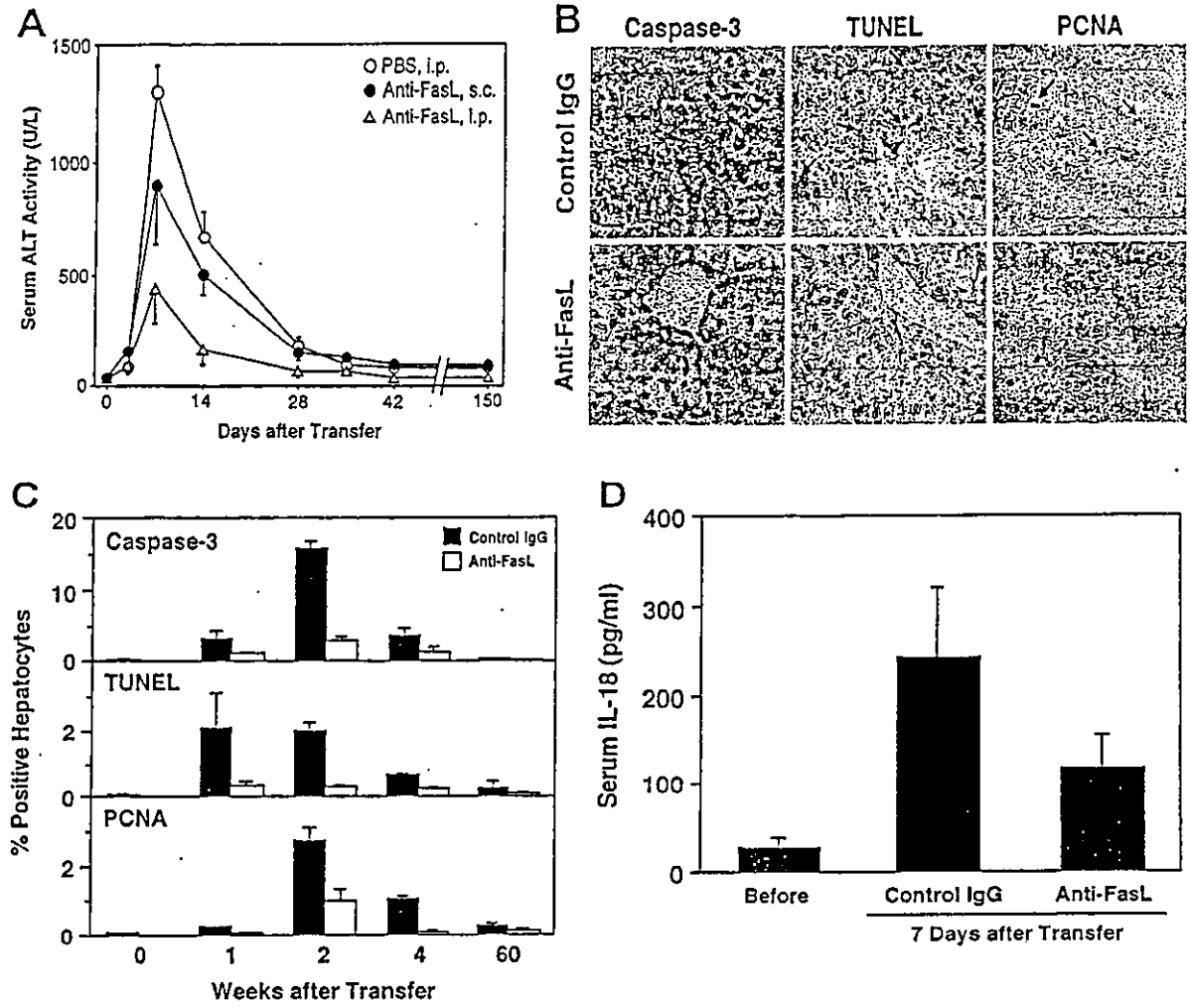


**Figure 1.** Anti-FasL mAb reduced hepatocellular apoptosis, inflammation, and regeneration in the prolonged acute-phase liver injury. (A) Anti-mouse FasL mAb or PBS was administered to HBsAg transgenic mice intraperitoneally or subcutaneously after the transfer of $5 \times 10^7$ HBsAg-primed nontransgenic splenocytes. Liver injury was evaluated by monitoring serum ALT activity. Vertical lines indicate standard errors. Each group represents five animals. Data shown represent three similar experiments. (B) Immunohistochemical analyses for active caspase-3, TUNEL, and PCNA were performed on liver sections from HBsAg transgenic mice that were treated with anti-FasL mAb or control hamster IgG, 14 d after the splenocyte transfer. TUNEL$^+$ and PCNA$^+$ hepatocyte nuclei are indicated with arrows. The bar represents 40 μm. (C) The proportions (%) of active caspase-3$^+$, TUNEL$^+$, or PCNA$^+$ hepatocytes were quantified in the transgenic mice that were treated with anti-FasL mAb (white bars) or control IgG (black bars) and killed at the indicated time points after the splenocyte transfer. Each group represents three animals. (D) The serum IL-18 levels before or 7 d after the splenocyte transfer were determined by ELISA.

the activation of IL-1β and IL-18 in neutrophils and macrophages, respectively, and that IL-18 is at least partly involved in the FasL-induced liver injury (19, 20). Serum IL-18 increased after the splenocyte transfer and anti-FasL mAb significantly reduced it (Fig. 1 D). These results indicate that anti-FasL mAb treatment inhibited inflammatory responses in this model. The anti-FasL mAb treatment also reduced the number of PCNA$^+$ hepatocytes, indicating suppression of the regenerative proliferation of hepatocytes (Fig. 1, B and C).

*Anti-FasL mAb Did Not Deplete CTLs.* CD8 CTL plays a primary role in the acute-phase liver injury in this animal model (reference 12, and unpublished data). Therefore, the reason that anti-FasL mAb protected the liver could be because it eliminated CTLs. To test this possibility, we compared the proportion of intrahepatic CD8$^+$ cells in control and anti-FasL mAb-treated mice at day 7. Approximately 15% of the IHLs were CD8$^+$ in transgenic mice that had been transfused with primed splenocytes (Table I). The anti-FasL mAb treatment did not reduce the proportion of CD8$^+$ cells. Interestingly, we reproducibly detected low but significant numbers of CD8$^+$ IHLs that produced IFN-γ in response to stimulation by the peptide representing residues 28–39 of HBsAg in transgenic mice transfused with primed splenocytes. This peptide is the major epitope of the HBsAg-specific CTLs detected in this model (12). Therefore, these IFN-γ–producing CD8$^+$ cells are likely to be the HBsAg-specific CTLs. The proportion